Submillimeter Astrophysics and Technology: A Symposium Honoring Thomas G. Phillips
*ASP Conference Series, Vol. **VOLUME**, **YEAR OF PUBLICATION***
D. C. Lis, J. E. Vaillancourt, P. F. Goldsmith, T. A. Bell, N. Z. Scoville, and J. Zmuidzinas

Heterodyne Receiver Development at the Caltech Submillimeter Observatory

J. W. Kooi

California Institute of Technology, MS 301-17, Pasadena, CA 91125

Abstract. The Caltech Submillimeter Observatory (CSO) operates at the summit of Mauna Kea, Hawaii, at an elevation of 4200 m. The site was chosen for its very dry climate and stable atmosphere, enabling submillimeter observations in the astrophysically important 1.3 mm to 300 μm atmospheric windows. Ever since its inception, the CSO has proven itself to be a productive test-bed for new detector technologies. In this paper we review the heterodyne (coherent) receiver development at the CSO, and highlight some of the ways it has helped to shape the field of submillimeter and terahertz high spectral resolution far-infrared astronomy.

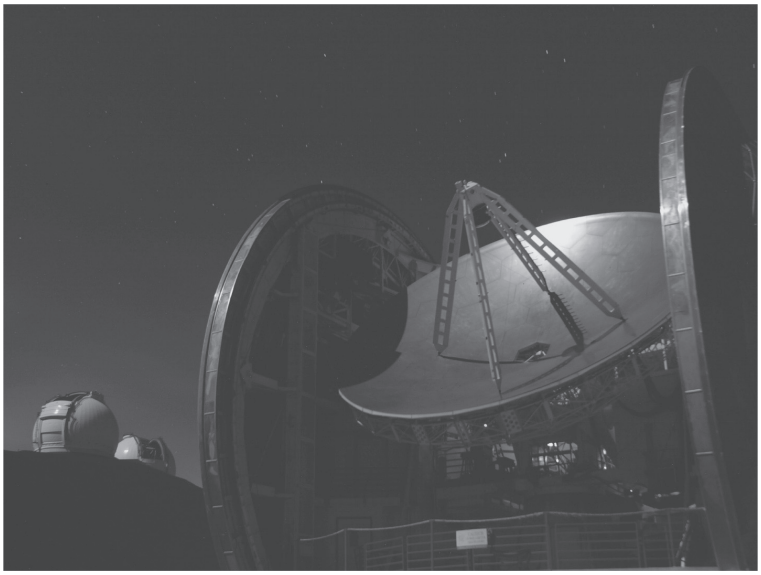

Figure 1. The Caltech Submillimeter Observatory (CSO) on top of Mauna Kea, Hawaii under full moon light. The 10.4 m diameter radio telescope was designed and assembled by a team led by Caltech Prof. Robert Leighton. In the background are the two Keck optical telescopes (10 m diameter, with hexagonal segment primary mirrors).

1. Introduction

The submillimeter band (1 mm – 100 μm) is an important one for astronomy. It contains spectral and spatial information on the cosmic background, on very distant newly formed galaxies, and on the early stages of star formation within gas clouds in our own galaxy. By 1973 technology had advanced enough to allow a proposal to the NSF by Prof. Robert Leighton to build four submillimeter telescopes, three as an interferometer at Owens Valley (California), and one on a yet to be determined high mountain site (Phillips 2007; Phillips & Keene 1992). Dr. Thomas Phillips, who was at the time at AT&T Bell Laboratories, New Jersey, joined the California Institute of Technology in 1980 as a Professor of Physics. Between 1982 – 1985 Prof. Phillips assumed duties as the associate director of the Owens Valley Radio Observatory (OVRO), with responsibility for millimeter-wave astronomy. In this same time-frame he continued research on low noise SIS mixers (Dolan et al. 1981) and together with Ed Sutton (Phillips's first postdoc at Caltech) and Dave Woody (OVRO) installed state of the art SIS receivers (Phillips & Woody 1982; Sutton 1983; Woody, Wengler, & Miller 1985) on the new OVRO telescopes, all the while doing site studies for what would become known as the Caltech Submillimeter Observatory (CSO). In those early days Prof. Phillips also organized an energetic group of PhD students (Elliott Brown, PhD 1985; Geoffrey Blake, PhD 1985; Mike Wengler, PhD 1987; Eric Grossman, PhD 1988; J. Stern, PhD 1990)[1] who, together with Dave Woody, continued to push the limits of SIS mixer technology (Wengler et al. 1985; Woody et al. 1985; Wengler & Woody 1987). The CSO was eventually established on top of Mauna Kea (Fig. 1), a 4200 m dormant volcano in Hawaii, USA. The choice of Mauna Kea was motivated by low precipitable water vapor conditions and convenient logistics from Pasadena, California. After some initial funding hurdles the observatory design and construction was officially started in 1983 with the facility inaugurated in November 1986 (Fig. 28; Phillips 2007). At this point Prof. Phillips assumed official responsibility as the Director of the CSO.

From its early beginning Prof. Phillips was a strong proponent of sensor technology development, both in the area of bolometers and coherent detectors. This followed a rich career in experimental astrophysics, amongst others, on the Kuiper Airborne Observatory (KAO), a US national facility operated by NASA to support research in infrared astronomy, and OVRO.

In practical terms, the push for high spectral resolution ($R \geq 10^6$) astrophysics required highly sensitive receivers approaching the quantum noise limit. To make this a reality, research focused on the development of superconducting-insulator-superconducting (SIS) heterodyne mixer technology with bandgap energies comparable to that of the to-be-detected (low energy) submillimeter phonons. Direct detector technology (bolometers) was also actively pushed forward by Prof. Phillips in the early 1990s with graduate students T. Hunter (PhD 1997) and D. Benford (PhD 1999). Noting that the sensitivity limit of ground based

[1]Elliott Brown is currently a professor of Electrical and Computer Engineering at the University of California Santa Barbara, Geoffrey Blake a professor of Cosmochemistry, Planetary Science, and Chemistry at the California Institute of Technology, Mike Wengler with Qualcomm in San Diego, Eric Grossman with NIST in Boulder Colorado, and Jeffrey Stern with the Jet Propulsion Laboratory (JPL).

direct detectors is primarily a function of atmospheric opacity and emissivity of the warm telescope optics, it was realized that significant gains in scientific throughput could only be obtained by arraying a large number of pixels. Thus the emphasis in Prof. Phillips's submillimeter group was primarily on increasing pixel count. This was successfully achieved with, for example, SHARC I (32 pixels; Wang et al. 1996) and SHARC II (384 pixels; Dowell et al. 2003, see also Dowell et al., this volume).

In this article we provide an overview of the heterodyne (receiver) instrumentation development in Prof. Phillips's submillimeter physics group at Caltech from approximately 1982 to the present. To provide a human face to the story emphasis is also given to the people involved. As we shall see, much has changed since the early days of SIS mixer design (Fig. 2), and in many ways this is the contribution of Prof. Phillips to the field of submillimeter technology, fundamentally stemming forth out of his desire for scientific advancement and education.

2. The Early Period (1982–1990)

2.1. E. Sutton, D. Woody, M. Wengler, R. Miller, and T. Büttgenbach

The history of heterodyne receiver development at the CSO starts with Ed Sutton, Dave Woody, Mike Wengler, and Ron Miller. Thomas Büttgenbach joined the group in 1986, around the time Mike Wengler was finishing up his doctoral research.

Mike was one of Tom's first graduate students at Caltech, and together with Dave Woody (OVRO) and Ron Miller (AT&T Bell labs) developed the first quasi-optical based bow-tie antenna SIS mixers. The antenna design was done in collaboration with Prof. Rutledge's group at Caltech (Rutledge et al. 1984). The superconducting mixers employed $0.3\,\mu\mathrm{m}^2$ ($\mathrm{J}_c = 10\,\mathrm{kA}^2\,\mu\mathrm{m}^{-2}$) $\mathrm{Pb_{90}In_8Au_2}$ lead-alloy SIS junctions and were fabricated by Ron Miller at AT&T Bell labs. With some good fortune the lifetime of these devices, when stored in a desiccator, was on the order of a few months at room temperature, and frequently less. In Figure 2*a* we show the quasi-optical mixer outline of Wengler et al. (1985). Two lenses are employed to focus the incoming radiation ($\sim f/4$) to the SIS tunnel junction. In Figure 2*b* the LO pumped, unpumped I/V curves are overlaid on the IF output power response to a warm (290 K) and cold (80 K) input load. This method is known as the Y-factor method and determines the sensitivity of the mixer, which was approximately 175 K double sideband (DSB) at 225 GHz, excellent at the time. Note that two 25 Ω Pb junctions are biased in series providing a gap voltage of ∼4.5 mV. The quasi-optical bowtie antenna of Wengler was experimental in nature, and suffered from a somewhat low coupling efficiency (Wengler et al. 1985; Wengler & Woody 1987).

Also in the early 1990s, between flying lessons and driving his red convertible Cadillac, graduate student Thomas Büttgenbach followed up on this work with more efficient dipole and log-spiral (silicon and quartz substrate) hyper-hemispherical open structure lens antenna designs (Buttgenbach et al. 1988). With these designs, operating frequencies were pushed well into the submillimeter wavelength regime (C $\mathrm{I}_{J=1-0}$, 492 GHz). The real breakthrough in

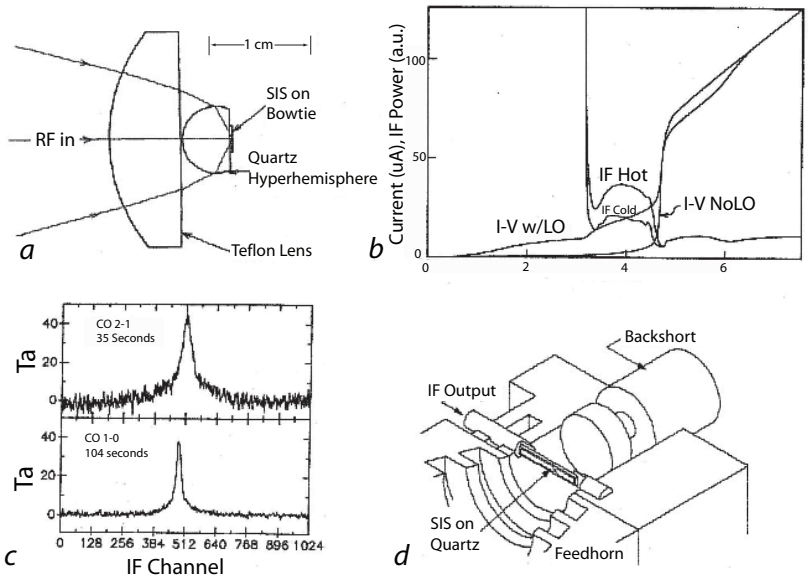

Figure 2. *a*) Quasi-optical layout of Wengler's mixer. The hyperhemispherical lens is made of quartz ($\epsilon_r = 3.8$). *b*) The LO pumped and unpumped I/V curves are overlaid with the IF output power response to a warm (290 K) and cold (80 K) input load; $T_{\rm rec}({\rm DSB}) = 175\,{\rm K}$. Two junctions are biased in series, giving a gap voltage of $\sim 4.5\,{\rm mV}$. *c*) OVRO observation with Wengler's quasi-optical bowtie antenna design of $^{12}{\rm CO}_{J=1-0}$ and $^{12}{\rm CO}_{J=2-1}$ at 115.268 and 230.531 GHz, respectively. Coupling efficiency to the telescope was $\sim$60 %, which when all things considered was quite good. The backend channel spacing is 500 kHz. *d*) Circular waveguide layout by Sutton (1983). The substrate is quartz and the movable backshort optimizes coupling to the SIS tunnel junction.

quasi-optical mixer design occurred, however, in 1992 with the introduction of the twin-slot mixer by Belitsky et al. (1992) and Zmuidzinas & LeDuc (1992). But we are now getting ahead of ourselves.

It should be noted that there were successful observations at OVRO with the experimental quasi-optical bowtie antenna of Wengler & Woody (Fig. 2*a*) in 1987. Both the $^{12}{\rm CO}_{J=1-0}$ and $^{12}{\rm CO}_{J=2-1}$ transitions were successfully observed as shown in Figure 2*c*. The coupling efficiency of the bowtie antenna was $\sim 60\%$ encouraging follow-up research, as discussed.

More or less synchronously, sensitive SIS mixers with high quality beam profiles and coupling efficiency were under development for the new OVRO telescopes. Sutton and Woody et al. (Sutton 1983; Woody et al. 1985; Woody, Giovanine, & Miller 1989) had taken up this challenge by developing waveguide SIS mixers for the 115 and 230 GHz atmospheric windows, an early layout of which is shown in Figure 2*d*. The initial design employed a circular waveguide (Sutton 1983), however it was soon realized that single mode rectangular waveguide with suitable impedance transformation would perform better. A movable backshort, similar to the one shown in Figure 2*d* optimized coupling to the superconducting lead-alloy tunnel junction. The SIS junction itself was situated at the midpoint of a bow-tie antenna that was carefully located in the center of

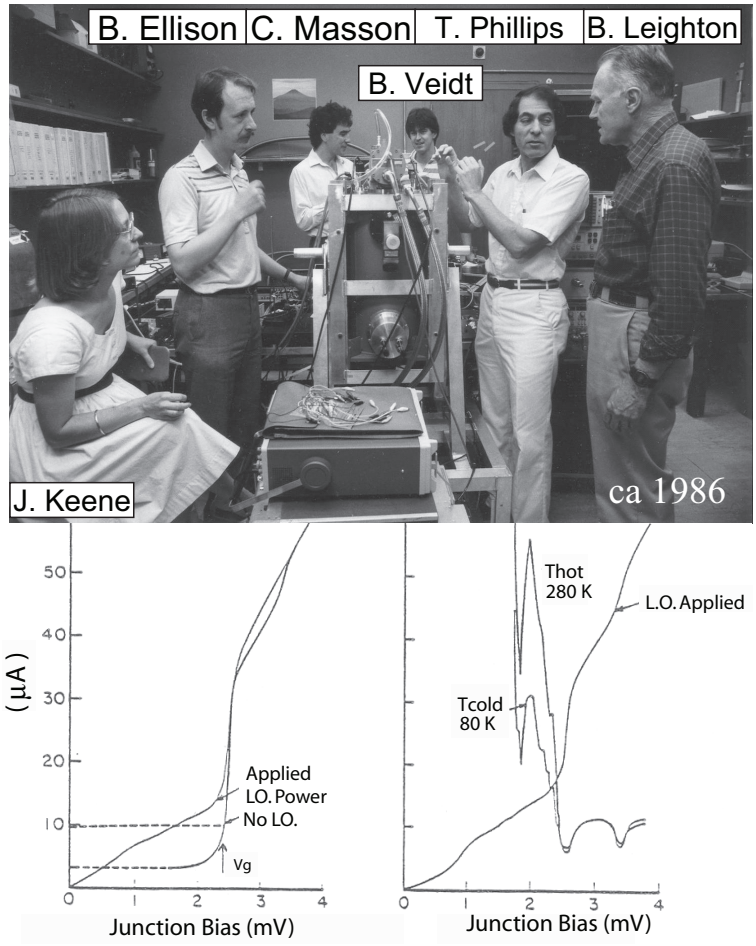

Figure 3. *Top:* Discussion around a successful demonstration of the CSO's first 230 GHz receiver. From left to right: Jocelyne Keene (postdoc), Brian Ellison (Engineer), Colin Masson (Scientist), Bruce Veidt (Engineer), Tom Phillips (Prof), and Bob Leighton (Prof). Location: Caltech's Downs Physics Laboratory, 4^{th} floor. Date: ca. 1986. *Bottom Left:* LO pumped and unpumped I/V curve. The $Pb_{90}In_8Au_2$ SIS junction was situated in the center of a full height waveguide at the apex of a bowtie antenna pickup probe. The double DSB receiver noise temperature was 114 K ± 15 K at 228 GHz. Similarly good performance was demonstrated between 200 – 290 GHz.

the waveguide. The substrate material is Z-cut quartz. As an interesting historical site note, Caltech Prof. Geoffrey Blake's doctoral research (PhD 1985) on Orion A at OVRO employed Sutton's circular waveguide design (Sutton et al. 1985; Blake et al. 1986).

2.2. B. Ellison, B. Veidt, and C. Masson

Once the CSO was formally approved and construction imminent (inauguration December 1986), there was a need to ready sensitive SIS receivers. The concept ($\sim$ 1985) was to house improved versions of the 115 GHz and 230 GHz full-height

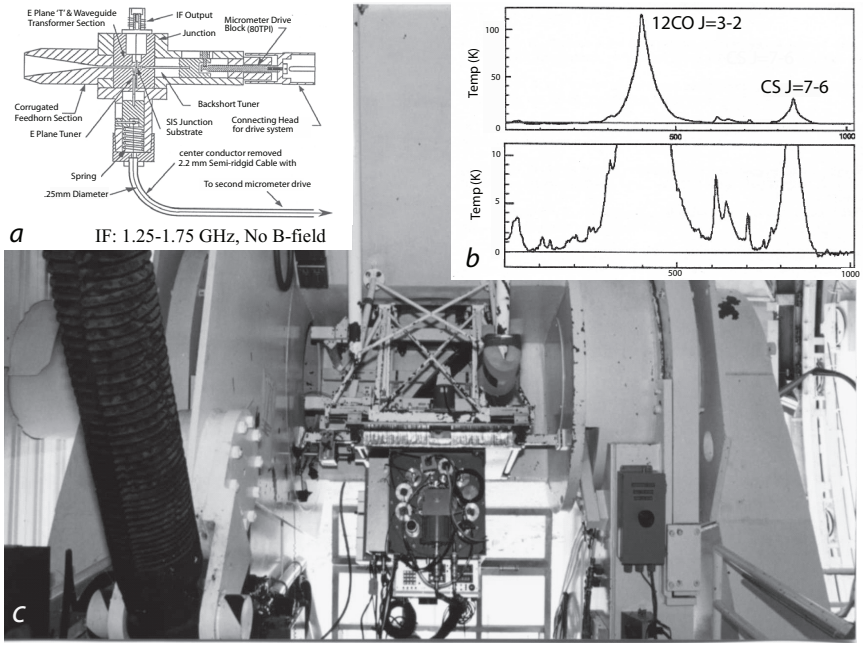

Figure 4. *a*) Schematic diagram of the 345 GHz mixer including backshort and E-plane tuner. *b*) $^{12}CO_{J=3-2}$ and $CS_{J=7-6}$ observations on Orion. *c*) The 345 GHz receiver (cryostat) installed at the Cassegrain area of the Caltech Submillimeter Observatory in December 1989.

waveguide mixers, in use at OVRO, in a single cryostat[2] at the observatory's Nasmyth focus. Brian Ellison (Fig. 3) was in charge of the receiver design and construction.

In his efforts Brian Ellison was assisted by Bruce Veidt, who had joined the CSO in 1984, and astrophysicist Colin Masson. Bruce worked, amongst other things, on the 1.25 – 1.75 GHz low-noise GaAs cryogenic amplifiers and a 500 MHz bandwidth acousto-optical spectrometer backend.[3] Also present at the time was Jocelyn Keene [postdoc, PhD U. Chicago (1980)].

Ellison's 115 GHz and 230 GHz mixer designs employed again $Pb_{90}In_8Au_2$ SIS junctions (R. E. Miller), had an E-plane tuner to further optimize coupling the SIS tunnel junction, and used a 64 section corrugated feedhorn with a frequency independent $f/D = 2.4$ single mode Gaussian beam. No magnetic field, required to suppress Josephson currents (Josephson 1962), had been incorporated in the mixer block, being at a sufficiently low frequency (Ellison & Miller 1987). The mixer blocks were fabricated by Custom Microwave Inc. (CMI)[4] and had a 500 MHz IF passband. One of the ironies of the 115 GHz mixer was

[2]Precision Cryogenics, http://www.precisioncryo.com/

[3]B. Ellison is currently with the Rutherford Appleton Laboratory, UK, and B. Veidt with the National Research Council of Canada.

[4]Custom Microwave Inc., http://www.custommicrowave.com/

that with the success and the demand for 230 GHz receiver observing time the 115 GHz mixer never really got turned on. So on one of the instrument servicing missions by the author the 115 GHz mixer was removed and provided to PhD student Rob Schoelkopf for his work on noise in Josephson effect mixers (Section 2.3.).

Following this success, a second Precision Cryogenics cryostat (assembled by a young National Guard reservist, P. L. Schaffer) and scaled-up 345 GHz mixer were procured. The 345 GHz receiver, again with a lead-alloy junction from R. Miller/AT&T Bell labs, exhibited a best DSB noise temperature response of 150 K ± 20 K on the telescope. Additional measurements showed that the receiver had an excellent response within an RF input range of 280 to 363 GHz. Figure 4*a* shows a schematic drawing of the 345 GHz mixer, complete with E-plane tuner, backshort, and feedhorn (Ellison et al. 1989). In Figure 4*b* we show $^{12}CO_{J=3-2}$ and $CS_{J=7-6}$ spectra from the Orion molecular cloud obtained with the 345 GHz Ellison receiver. The bottom photograph shows the 345 GHz receiver installed at the CSO in December 1989 when the author first joined the CSO. Note that even back then, only three years after the inauguration, the Cassegrain focus area already looked heavily used with paint flaking off. Some things never change.

2.3. R. Schoelkopf

As was mentioned in the previous section, the essentially unused 115 GHz Ellison waveguide mixer was pulled out of the 115/230 GHz cryostat in 1990 and provided to Rob Schoelkopf (PhD 1994)[5] to assist him with his studies of "noise in Josephson-effect mixers and their potential for submillimeter heterodyne detection." Schoelkopf's 115 GHz Josephson mixer (Josephson 1962) complete with E-plane tuner, backshort, and original lens is shown in Figure 5*a*. Some other students in Prof. Phillips's group at that time were T. Groesbeck (PhD 1994) with whom Rob shared an office, K. Young, a.k.a. Taco (PhD 1993), and previously mentioned T. Hunter (PhD 1997), and D. Benford (PhD 1999). PhD students John Ward (PhD 2001), Attila Kovács (PhD 2006), and Min Yang (PhD 2007) came later.

Fundamentally, Schoelkopf's thesis describes the theoretical and experimental investigation into the noise processes of Josephson junctions, with the intent of evaluating their potential as heterodyne mixers in the frequency range from 300 GHz to 3 THz. Theoretical modeling, based on the resistively shunted junction (RSJ) model, indicates the presence of excess noise. The source of this excess noise was found to be Josephson oscillations, which being completely incoherent, result in linewidth comparable to the operating frequency. Hence AC Josephson oscillations appear in the mixer as an intrinsic broadband noise source. Nevertheless, sensitivity levels of an optimized Josephson mixer were intriguing, as shown in Figure 5*c*, with measured receiver noise temperatures as low as 190 K (DSB). Mixer conversion efficiency at 102 GHz was −6 dB (Schoelkopf 1994). It should be noted that these results are still a factor of four higher than those predicted by the RSJ simulations, and were shown by Schoelkopf to be

[5]Rob Schoelkopf is presently a professor of applied physics at Yale University.

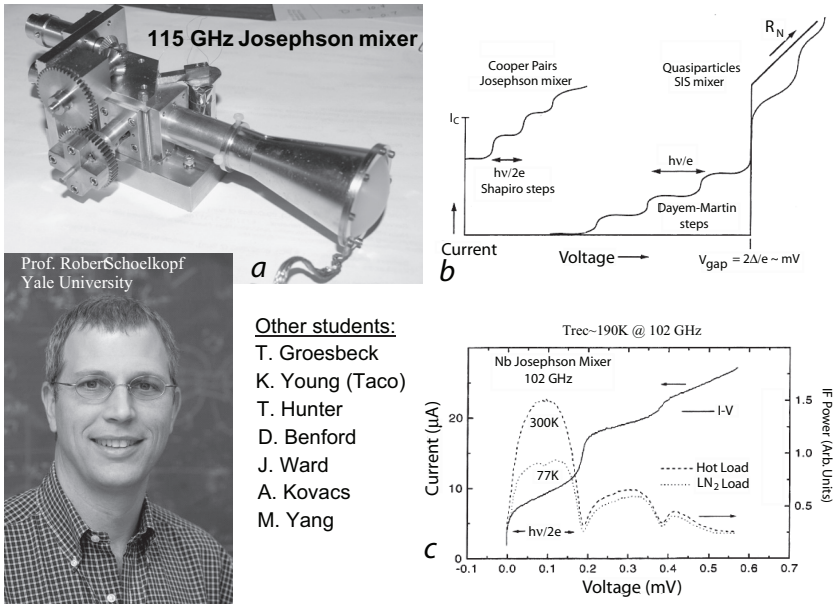

Figure 5. *a*) Full height waveguide mixer block with adjustable E-plane and backshort tuners used in Schoelkopf's Josephson experiments. *b*) Current-Voltage characteristics of a superconducting tunnel junction. The Shapiro steps (Shapiro & Little 1963), due to photon assisted tunneling of Cooper pairs (Bardeen, Cooper, & Schrieffer 1957) move out from zero voltage and have a width of $\Delta V = h\nu/2e$. The Dayem-Martin steps (Dayem & Martin 1962), caused by photon assisted tunneling of quasiparticles, move out from the gap voltage, and have a width of $\Delta V = h\nu/e$. *c*) Total power response of the Nb based Josephson mixer at 102 GHz. Optimum Y-factor was 1.82, corresponding to a DSB system noise temperature of 190 K.

the result of a nonlinear interaction between the junction and RF embedding circuit, making it very difficult to achieve the theoretical noise limit.

3. The Nineties

3.1. The First Nb-based SIS Mixers

Around 1990 the first niobium SIS junctions became available from JPL's micro-device group. With a higher gap voltage (2.8 mV) than the lead-alloy SIS junctions of Section 2.2., a reduced gap smear (typically $\pm 50\,\mu$V), lower leakage current (subgap/normal-state resistance ~ 20), and increased chemical robustness came the promise of higher conversion efficiency and improved sensitivity. To put the new Nb devices on the telescope as quickly as possible it was decided (Phillips, Zmuidzinas, Kooi) to replace the Pb based SIS junction in Ellison's 230 GHz mixer (Fig. 3) with a Nb tunnel junction; the RF choke, substrate, and bowtie antenna being the same.

However, more IF bandwidth was desired, and to further improve the performance with the 230 GHz mixer block a 1 – 2 GHz IF passband matching

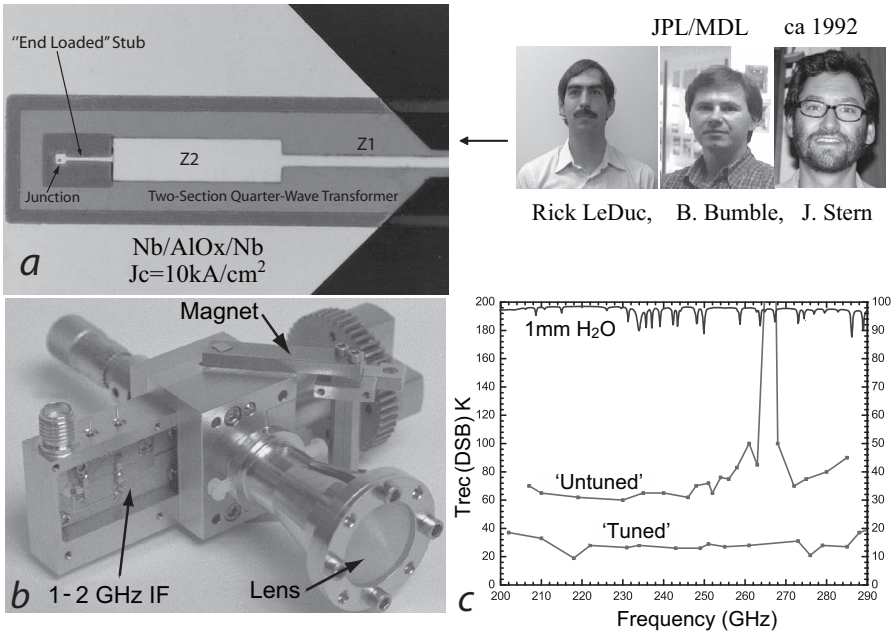

Figure 6. *a*) Layout of a 230 GHz 'end-loaded stub' RF matching network and SIS junction. The geometric capacitance of the SIS tunnel junction is tuned-out by a series inductor. The resulting low impedance is then transformed to match the waveguide probe impedance by means of a two-section Chebyshev quarter-wave transformer. The devices were made at the micro device laboratory (MDL) of JPL. *b*) 230 GHz mixer block with backshort, E-plane tuner, magnetic field concentrators to suppress the Josephson effect, and integrated 1 – 2 GHz IF match/bias network. *c*) Performance of an 'untuned' and 'tuned' SIS junction. In both cases a bowtie antenna, located in the center of a full height rectangular waveguide, is used to pick off the signal.

network with integrated bias tee was introduced (Kooi et al. 1992; Fig. 6*c*). The performance of the untuned device is shown in Figure 6*d*.

Further improvements were made in 1994 with the introduction of on-chip RF tuning to compensate the relatively large geometric junction capacitance (Kooi et al. 1995). Also added to the block were high permeability magnetic field concentrators to facilitate suppression of Josephson oscillations (Walker et al. 1992). In Figure 6*a* we show an 'end-loaded stub' RF matching network with the Nb SIS junction located inside the 5×5 μm^2 area (facilitates alignment). The responsible parties for making the excellent devices are shown to the right (R. LeDuc, B. Bumble, J. Stern, all from JPL). Clearly the progressive improvement from an untuned $Pb_{90}In_8Au_2$ lead-alloy SIS junction ($T_{\rm rec}$(DSB) $\sim$ 115 K) to a RF-tuned Nb SIS tunnel junction is impressive ($T_{\rm rec}$(DSB) $\sim$ 35 K, or $\sim$ 3 times $h\nu/k_B$). It is at this level that the front-end optics loss really starts to dominate the noise budget.

3.2. C. K. Walker

C. K. Walker was a Millikan Fellow at Caltech (Phillips's group) from 1989 to 1992. His area of research focused on submillimeter heterodyne technology. As

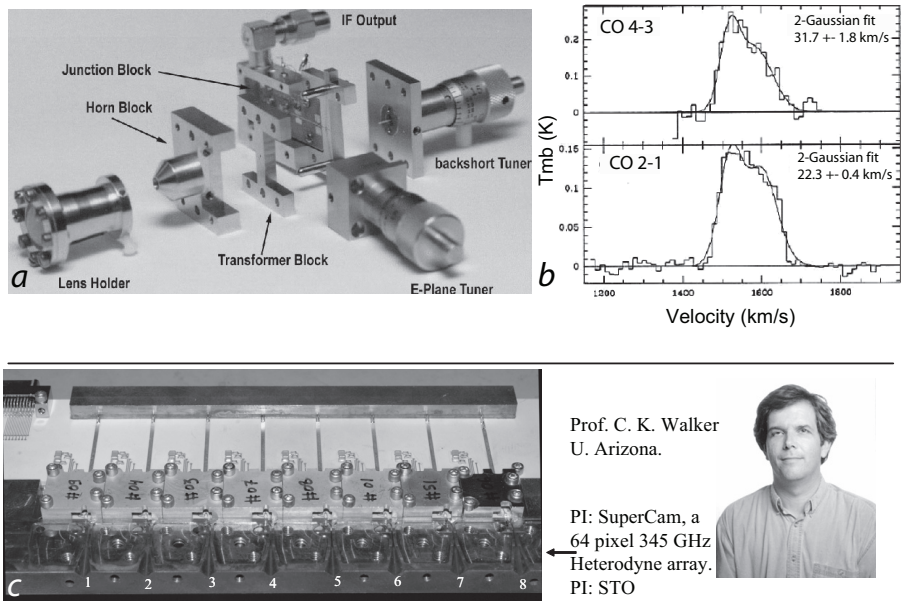

Figure 7. *a*) The 492 GHz full-height mixer block by Walker et al. The DSB receiver noise temperature at 461 GHz was 170 K. *b*) $^{12}CO_{J=4-3}$ and $^{12}CO_{J=2-1}$ spectra of M100 (NGC4321) the Virgo Cluster with the same mixer, but upgraded to a 'tuned' junction. At the velocity of this galaxy this corresponds to central frequencies of 458.7 and 229.3 GHz, respectively. System temperatures and approximate zenith atmospheric transmissions were 2000 K (0.04) at the $J = 4 - 3$ frequency and 200 K (0.95) at the $J = 2 - 1$ frequency. *c*) Detailed view of a 1×8 SuperCam sub-array. LO and RF signals enter the front of the mixer block via eight pyramidal horns. Eight superconducting magnets are integrated at the backside of the block (not visible). These allow the magnetic field for each junction to be set individually. The IF signals, after ~ 35 dB "on board" MMIC amplification (S. Weinreb's group at Caltech) are taken out toward the rear of the sub-array. At this same interface plane SIS mixer, MMIC, and magnet bias signals enter the IF circuit board.

such he pushed waveguide mixer technology forward with the 400 – 520 GHz SIS mixer of Figure 7*a*. The mixer block was made of a corrugated feedhorn block, circular-to-rectangular waveguide transformer block, E-plane tuner block, junction and IF matching/bias network block, and adjustable backshort tuner block. The first 492 GHz SIS junctions were of the 'untuned' niobium kind (Walker et al. 1992) as described in Section 2.2., a few years later to be upgraded to an 'end-loaded stub' tuned SIS junction design (Kooi et al. 1995).

Important in Walker's design is the introduction of magnetic field concentrators which are needed to suppress Cooper pair tunneling (Josephson effect) across the barrier. At 492 GHz (C $I_{J=1-0}$) the first Shapiro step is at 2.1 mV ($h\nu$/2e) and is located in the middle of the first phonon step ($h\nu$/e) below the gap, thus prohibiting quasi-particle operation were it not for proper suppression of the Josephson effect. The receiver achieved a DSB noise temperature of 170 K

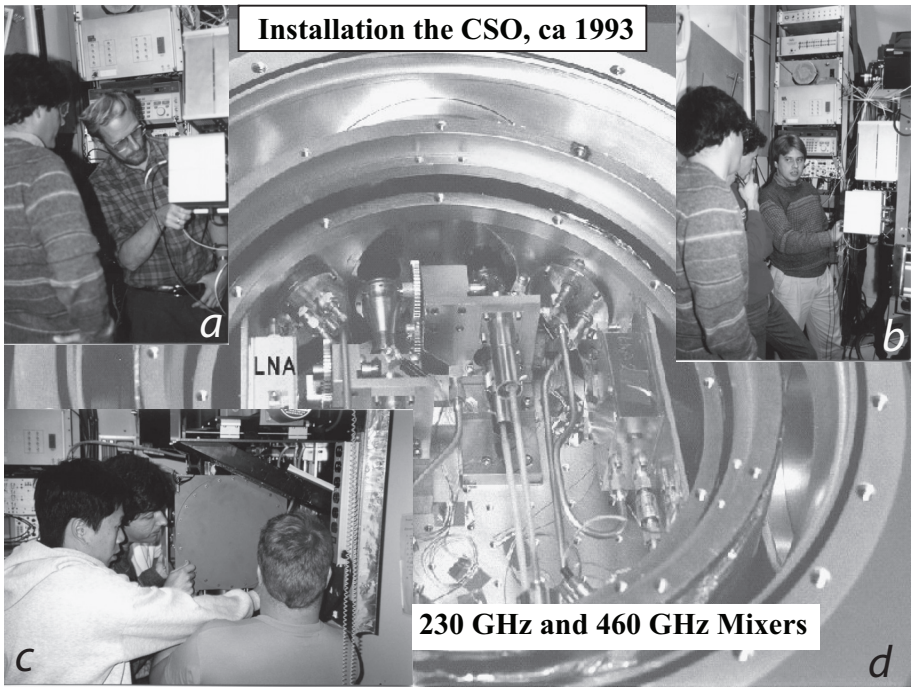

Figure 8. Internals of the 230/460 GHz dewar. Note the backshort and E-plane tuners. The balanced LNA's have a low input/output return loss (−15 dB) and approximately 35 dB of gain (GaAs HEMTs). *a*) Chris Walker and Jacob Kooi biasing the newly installed 492 GHz receiver (1992). *b*) Jonas Zmuidzinas explaining single electron quasi-particle tunneling, overlapping wave functions, and the nasties of Cooper pair tunneling at 4200 m. *c*) Benson Chan, Chris Walker, and Pat Schaffer juggling the upgraded 230/460 GHz cryostat.

at 492 GHz. Figure 7*b* shows a $^{12}CO_{J=4-3}$ (460 GHz) and $^{12}CO_{J=2-1}$ (230 GHz) spectrum of M100, a spiral galaxy in the Virgo Cluster, taken at the CSO.

After his Millikan Fellowship (postdoc) period at Caltech, Dr. Walker accepted a faculty position at the University of Arizona Radio Astronomy Laboratory (SORAL). His group has pioneered multi-pixel submillimeter heterodyne array receiver technology. SuperCam (Groppi et al. 2006) is a 64 pixel heterodyne camera designed for operation in the astrophysically important 870 μm atmospheric window at the 10 m Heinrich Hertz Telescope (HHT), and is the latest in a series of a progressively larger and more complex instrument designs at SORAL.

It is interesting to note that while the possibility of such heterodyne arrays has been discussed for more than two decades, amongst others by Prof. Phillips (Gillespie & Phillips 1979), only recently have advances in mixer technology, device fabrication, micromachining, and digital signal processing made this concept a reality.

Figure 8 shows the installation of the 230/460 GHz cryostat at the CSO in 1992. The 230 GHz lead-alloy SIS tunnel junction mixer and electronics of Section 2.2. were upgraded to accommodate niobium based 230/460 GHz mixers,

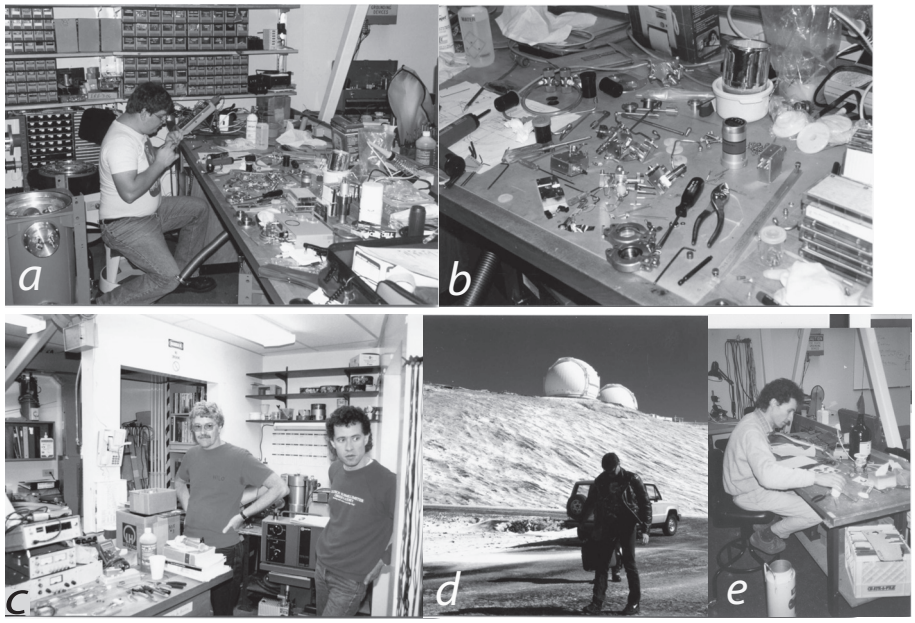

Figure 9. *a*) Pat Schaffer reworking the 345 GHz cryostat after years of frustration with unreliable bias connectors. Date: December 1995. *b*) Cryostat and mixer hardware carefully laid out in the observatory's receiver room. *c*) Brian Force and Antony Schinkel surveying the progress. *d*) T. J. Creath enjoying paradise. The two Keck observatories in the background. *e*) Antony Schinkel making circular Eccosorb disks for beam pattern measurements.

of the 'untuned' type. The IF bandwidth was at the time also upgraded, from 500 MHz to 1 GHz, to be compatible with the 1 – 2 GHz balanced low noise amplifiers of Padin & Ortiz (1991). Figure 8*a* shows C. Walker and J. Kooi busy at work tuning the receiver. Figure 8*b* depicts J. Zmuidzinas explaining quantum mechanics at 4200 meters, amazingly well one may add. In the middle is A. Schinkel, at the time the technical director of the CSO. Later he joined the Harvard-Smithsonian Submillimeter Array (SMA). At the bottom of the figure we see Benson Chan (Engineer), Pat Schaffer (Technician), and Chris Walker (postdoc) juggling the cryostat.

3.3. Reworking of the 345 GHz Cryostat at 4200 m

Of course not all went perfectly and smoothly. One of the very annoying difficulties encountered were the bias feedthrough connectors on the 12 K stage. After a number of thermal cycles and extended period in the cold they became unreliable (the company shall not be named here). At some point the only option left was to replace all of the connectors with a different type, but this meant taking the entire cryostat apart. Unfortunately the CSO office was at the time ($\sim$ 1995) located at the bottom of a dentist office in Hilo, in close proximity to Cafe 100. This tropical setting did not lend itself to such a difficult and clean operation, and the operation was performed at the observatory in thin air.

In Figure 9*a* we show Pat Schaffer with a completely disassembled cryostat.

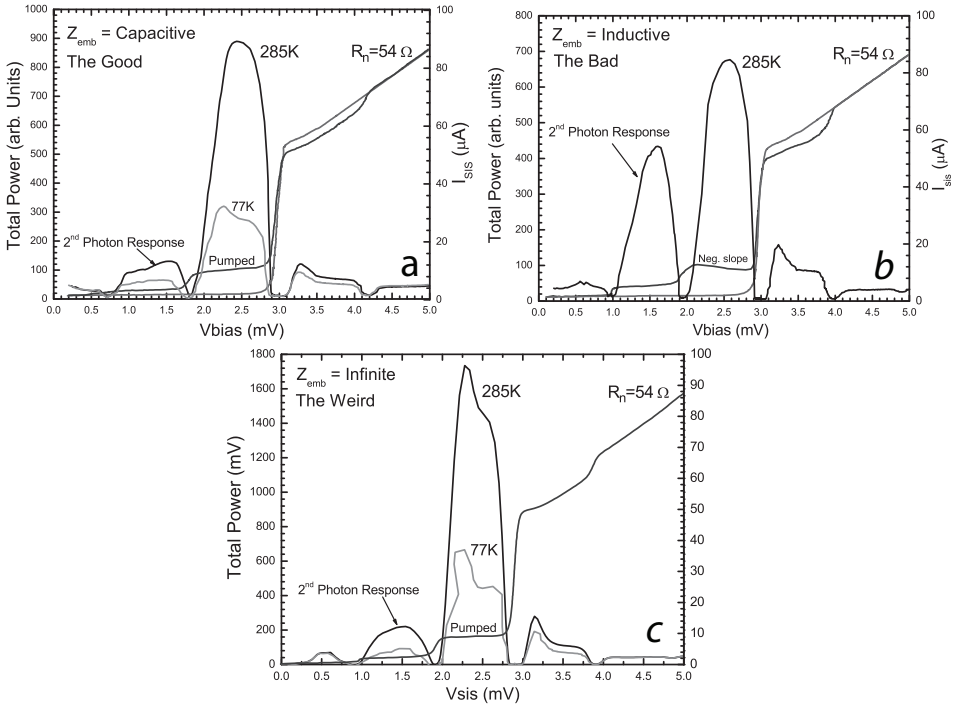

Figure 10. *a*) An example of a properly tuned mixer. In this case the subgap I/V curve is positive which is indicative of a capacitive embedding impedance at the SIS junction. *b*) Improper tuning, the negative subgap I/V curve slope indicates an inductive SIS junction embedding impedance. This condition can lead to conversion gain (due to the quantum nature of the quasiparticle tunnel current) and unstable mixer behavior. *c*) Improper tuning, the infinite subgap I/V curve slope causes similarly unstable mixer behavior.

Words cannot really describe his excitement. Figure 9*b* gives a closer view of the carefully laid out mixer components with Brian Force and Antony Schinkel always willing to provide a helping hand (Figs. 9*c* and 9*e*). In Figure 9*d* we find T. J. Creath, the software guru who wrote all the code for the Octagon handheld receiver control displays, feel the ground outside the observatory. He never quite got over being in 'paradise'.

Other memorable events include an implosion of the 345 GHz Ellison dewar as ice was melted off the mylar pressure window by means of a heat gun (∼1992), the cooling of an un-evacuated cryostat, attempting to observe on a dummy load (which incidentally provides for very nice baselines), the use of a whisker contacted multiplier that at some point would only work at temperatures above +8 C in the middle of a freezing night, and attempts to observe with Eccosorb in the beam.

3.4. The Good, and not so Good of Tunable Heterodyne Receivers

The CSO, being a single dish telescope with emphases on experimental (hands-on) physics, has from its early beginning employed backshort and E-plane tunable mixers. Traditionally this was largely driven by the quest for optimal

sensitivity and difficulty in establishing a proper embedding impedance (Tucker 1979; Tucker & Feldman 1985) at the SIS junction interface. In the mid-1990s this style of tunable waveguide receivers slowly moved out of vogue as more sophisticated analysis tools (software) became available. Also around this timeframe the twin-slot quasi-optical (open structure) mixer (Belitsky et al. 1992; Zmuidzinas & LeDuc 1992; Zmuidzinas et al. 1994) was shown to have a high quality Gaussian beam, important for achieving good coupling efficiency to the telescope, and compatible sensitivity to waveguide mixers.

Having the ability to adjust the embedding impedance seen by the SIS tunnel junction provides, aside from being a nice educational tool, a mechanism for not only achieving proper tunings (Fig. 10*a*), but also quite interesting improper tunings (Fig. 10*b*), for example with infinite or negative sloped I/V curves. A negative I/V curve can result in conversion gain (a quantum mechanical phenomenon), unstable mixer behavior with related intensity calibration problems, essentially manifesting itself in significant IF baseline distortion. This is clearly a situation to be avoided. Inevitably there were the occasional odd tunings as shown in Figure 10*c*, some of which clearly related to the physiological effects of high altitude (4200 m).

Having the ability to 'tune' the receiver did on occasion have some practical significance as well. For example, in an act of scientific desperation it is possible to push the band edge frequencies and operate in an 'overmoded state'.

3.5. Social Events

Of course life at the observatory was not all hard work, being physically located in 'paradise'. For example, in Figure 11*a* we have the retirement party for Lynn Holt (Electronics/Software technician). From left to right we have: Prof. Tom Phillips, Diana Bisel (CSO assistant), and Lynn Holt. In Figure 11*b* the characters of play are Martin Houde (scientist), Prof. Tom Phillips, Lynn Holt, and Mac Cooper (Software Engineer), currently with the Harvard-Smithsonian Submillimeter Array (SMA).

Another event that comes to mind is a barbecue on Coconut island, Hilo, ca. 1996. To the left in the foreground are Antony Schinkel and T. J. Creath. Schinkel was the CSO technical director at the time and T. J. Creath a software engineer from Campus.[6] Also present at the beach party was Ken Young (Fig. 11*d*), a.k.a. Taco, who is currently with the SMA. Finally in Figure 11*e* we show Dave Vale (former Caltech based machinist) who together with Walt Schaal (not shown) did much of the initial work on the telescope design and construction. The three Caltech bases assistants Susan McCurdy, Sylvie Gertmenian, and Rena Becerra-Rasti are shown in Fig. 12.

[6]Current CSO technical director Richard Chamberlin took over Antony's position after he joined the Harvard-Smithsonian Submillimeter Array (SMA) in late 1996. T. J. Creath is with Microsoft.

Figure 11. *a*) Retirement party of Lynn Holt (2002). Shown are Prof. Phillips, Diana Bisel, and Lynn Holt. *b*) Also present at Lynn's retirement party were (from left to right) Martin Houde, Prof. Phillips, and Mac Cooper. *c*) Barbecue at Coconut island. *d*) Ken Young, a.k.a. Taco. Later he defected, along with Antony Schinkel and Mac Cooper, to the Harvard-Smithsonian Submillimeter Array (SMA). *e*) Dave Vale (machinist) who with Walt Schaal (Mechanical Engineer, not shown) did a lot of work on the early telescope construction and early instrumentation.

Figure 12. From left to right, the Caltech based assistants Susan McCurdy, Sylvie Gertmenian, and Rena Becerra-Rasti (2007). Without these ladies not much would get done.

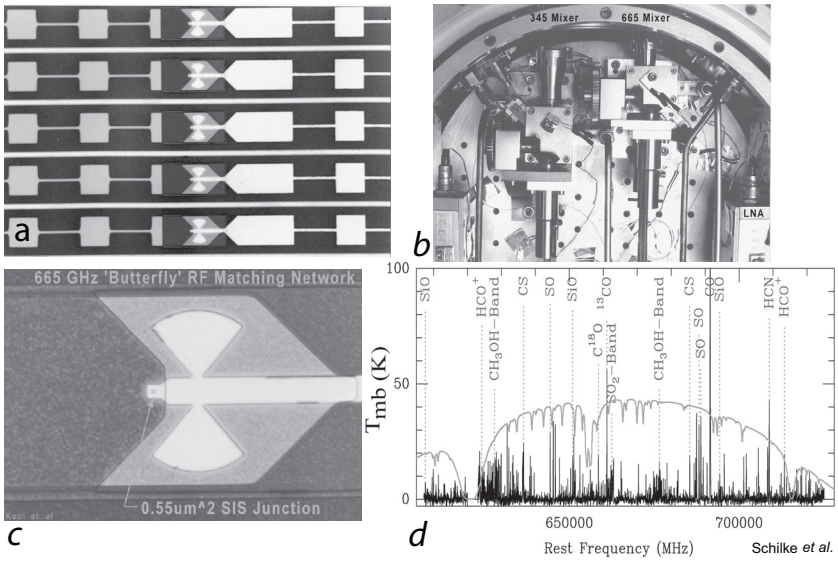

Figure 13. *a*) Mask layout of the 665 GHz AlO_x SIS tunnel junctions. Fabrication at MDL (JPL). *b*) Photograph of the 345/665 GHz cryostat. The 665 GHz mixer is to the right with its horn pushed all the way forward toward the 15 K stage. *c*) SEM picture of an 665 GHz mixer chip. The substrate is 50 μm thick Z-cut quartz. *d*) Spectral line survey in the frequency range 600 – 720 GHz by Schilke et al. (2001).

3.6. Moving to Higher Frequencies, the 600 – 720 GHz Receiver

By the mid-1990s there was a real push to higher (submillimeter) frequencies. One such effort is shown in Figure 13. The challenge in this frequency band is that at $\sim$ 690 GHz incident photons have enough energy to break Cooper pairs which results in a significant absorption loss in the superconducting Nb films.

A variety of RF matching networks have been proposed (Schuster, Harris, & Gundlach 1993; de Lange et al. 1994; Salez et al. 1994) to deal with this loss mechanism and the RF matching problem. The author and colleague Man Chan chose, after some linear circuit simulations, a less conventional butterfly design (Kooi et al. 1996). This is depicted in Figure 13*c*. The 600 – 720 GHz Orion-KL spectral line survey of Figure 13*d*, published by Schilke et al. (2001), is a nice example of the instrument's high spectral resolution capability.

3.7. The Next Challenge: 850 GHz

One of the problems of scaling the mixer dimensions to higher operating frequencies is that, aside from natural mechanical tolerance challenges, the junction substrate (quartz) becomes impractically thin. To circumvent this problem, we proposed in 1998 the use of 1 μm thick silicon nitride (Si_3N_4) membrane, supported by a silicon frame, for the newly designed 850 GHz waveguide SIS mixer (Kooi et al. 1998; Fig. 14). The mixer was acquired from CMI, again with the familiar two-tuner design. This would be the last of its kind, technology was moving on rendering mechanical tuner designs obsolete.

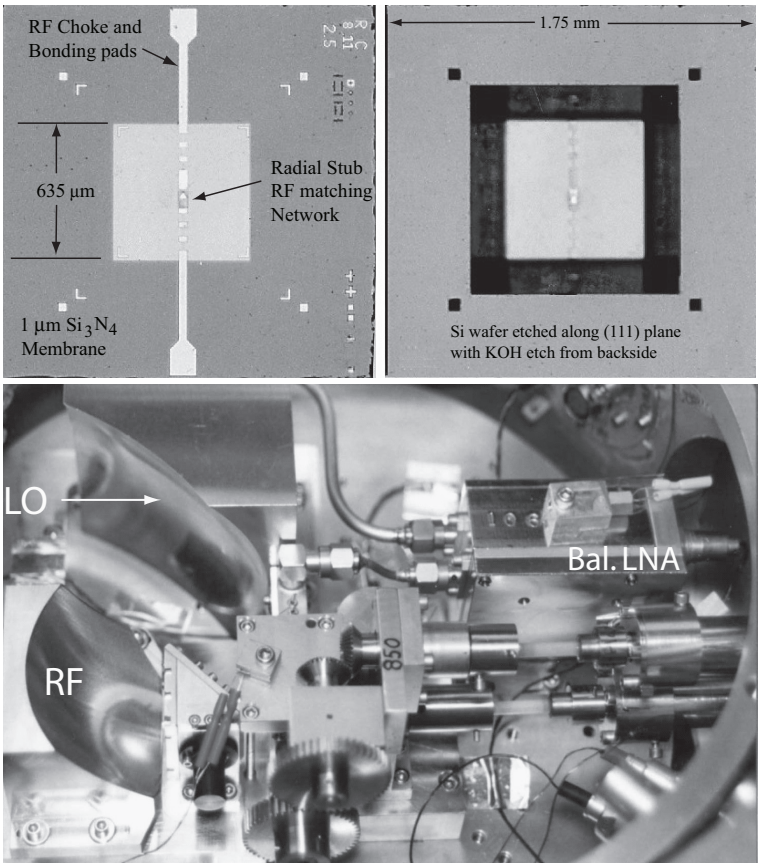

Figure 14. *Top:* 1 μm thick silicon nitride membrane with the bow-tie antenna and radial probe matching network on top of a 250 μm Si frame. The exposed (100) silicon areas on the back side are anisotropically etched in a bath of 30 % KOH solution at 70 C. Junction size is 0.55 μm × 0.55 μm with an AlO_x tunnel barrier and critical current density of 14 kA cm^{-2}. *Bottom:* Photograph of the 850 GHz waveguide mixer cryostat with all cooled optics.

Because the operation was entirely above the energy gap of Nb, the RF matching network between the antenna waveguide probe and SIS junction had to be as simple as possible, thereby minimizing film loss. The IF frequency was 1 – 2 GHz and used the balanced IF amplifier discussed earlier (Padin & Ortiz 1991). The signal and local oscillator chain uses all reflecting optics and was cryogenically cooled for the first time in CSO history (Fig. 14 *bottom*). This, in addition to anti-reflection coated quartz vacuum and infrared blocking windows (the Australian company that supplied the windows went out of business soon afterwards), helped minimize the front-end optics loss.

Bruce Bumble, responsible for fabrication of the Si_3N_4 membrane supported niobium SIS junctions, is shown in Figure 15*a* (left). Mac Cooper (right) helped out with the optical alignment and mirror motion control. In Figure 15*b* we show Allan Guyer in the process of installing the 850 GHz cryostat on the Cassegrain relay optics (Serabyn et al. 1994). Pat Nelson was controlling the crane. This

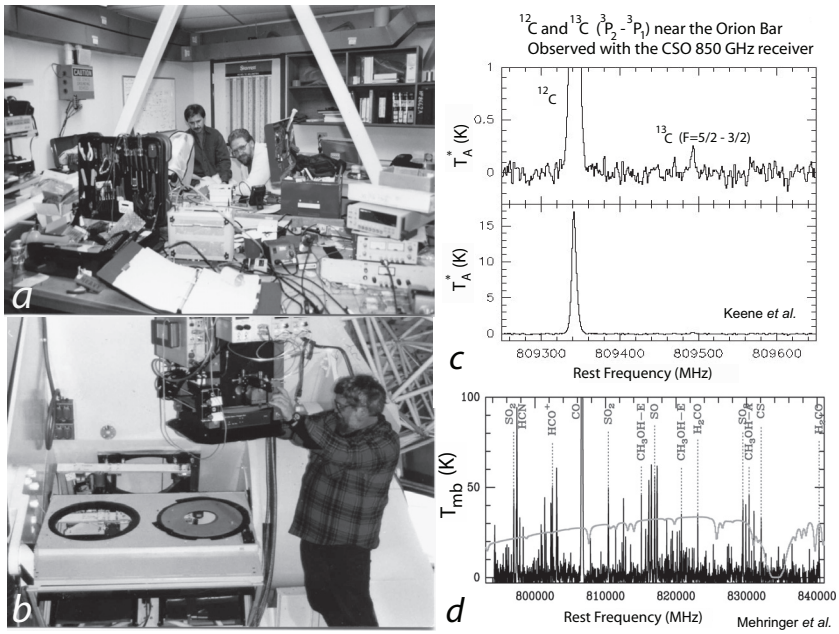

Figure 15. *a*) Bruce Bumble (left) and Mac Cooper assisting with the installation of the 850 GHz waveguide receiver. *b*) Allan Guyer installing the 850 GHz cryostat on the Cassegrain focus relay optics. *c*) ^{12}C and ^{13}C (^{3}P$_2$ – ^{3}P$_1$) detection near the Orion Bar region by J. Keene et al. *d*) 794 – 840 GHz Orion line survey by Mehringer et al. (1998).

receiver was the first of its kind to cover the important 800 – 950 GHz atmospheric window, and many new atomic, molecular, and isotopic lines could be observed for the first time. Examples include ^{12}C and ^{13}C (^{3}P$_2$ – ^{3}P$_1$) near the Orion Bar region by Keene et al. (1998; Fig. 15*c*) and the 794 – 840 GHz Orion line survey by Mehringer et al. (1998) in Figure 15*d*.

It should be noted that at that time (1998) there was no local oscillator available that operated in the frequency range 800 – 900 GHz. So at some point the author contacted Radiometer Physics[7] to see if such a LO could be built. The answer came back that it would take many tuning knobs. Knowing Prof. Phillips's fondness for optimizing the system performance by tuning all available knobs, the author was not too discouraged with the answer. Upon querying, Tom replied: "I do not care if it takes 20 knobs, just do it". I could never really imagine a 20 tuner local oscillator, however with some imagination it must have looked something like the one depicted in Figure 16*a*. To show the validity of this (true) story, we show in Figure 16*b* Prof. Phillips busy at work tuning one of the CSO sidecab receivers (photo courtesy R. Monje, January 2009).

[7]Radiometer Physics GmbH, http://www.radiometer-physics.de/rpg/html/Home.html

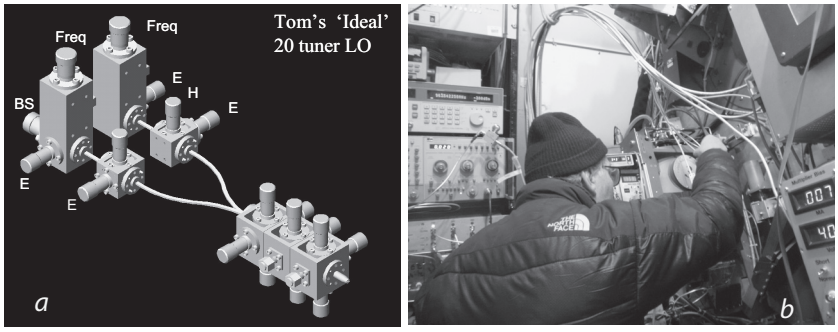

Figure 16. *Left:* Tom's "ideal" 20 tuner 850 GHz local oscillator. *Right:* Prof. Phillips tuning one of the sidecab receivers (January 2009).

3.8. A New Technology: NbTiN Films with AlN Junction Barriers

As suggested in Section 3.6., niobium has an energy gap ($2\Delta = h\nu$) of 690 GHz above which the film loss due to the breaking of Cooper pairs increases substantially. Thus for frequencies above $\sim$ 690 GHz higher energy gap (T_c) materials are desired. In 1998, driven in large part by mixer development for the high spectral resolution Heterodyne Instrument for the Far Infrared (HIFI) (de Graauw et al. 2006) on the Herschel Space Observatory (de Graauw & Helmich 2001), and the fact that Prof. Phillips is the US Principal Investigator (PI, 1998), an all NbTiN twin-slot open structure mixer was designed (J. W. Kooi, G. Chattopadhyay, J. Zmuidzinas). In the described design the actual SIS junctions were fabricated with an AlN tunnel barrier, Nb top electrode, and NbTiN counter electrode at JPL (R. LeDuc, B. Bumble, J. Stern). This design was fundamentally based on twin-slot antenna work by Prof. Zmuidzinas's group at Caltech (Gaidis et al. 1996; Bin 1997; Zmuidzinas et al. 1998).

With many of the NbTiN film properties unknown, the fabrication, testing, and re-design took some serious effort. Many wafer runs were made at JPL, with devices tested on a Fourier Transform Spectrometer (FTS) at Caltech. Assisting with this effort were Dr. J. Chen and postdoc J. Kawamura.[8] For the mask layout shown in Figure 17 both the top and bottom wire layers are NbTiN. It turned out that it was very difficult to grow a high quality (low temperature) epitaxial NbTiN top layer without degrading the quality of the SIS junction trilayer. Based on this experience, future devices would use Al as the wire layer (Jackson et al. 2006). The inset shows the calculated loss per wavelength for Nb, NbTiN, and Al films as a function of frequency (Kooi 2008).

As mentioned earlier, the junction barrier of the new devices was AlN which turned out to be chemically even more robust than AlO_x. And because the barrier could be made thinner, this also provides a mechanism to increase the junction current density without degradation of quality. Figures 18*a* and 18*b* show the all NbTiN twin-slot mixer block with the AR coated silicon lens. In Figure 18*c* we depict an alignment and focusing test of the cooled optics. The improvement of the all NbTiN receiver over the niobium based SIS waveguide

[8]Jonathan Kawamura is currently with the Jet Propulsion Laboratory, Pasadena, California

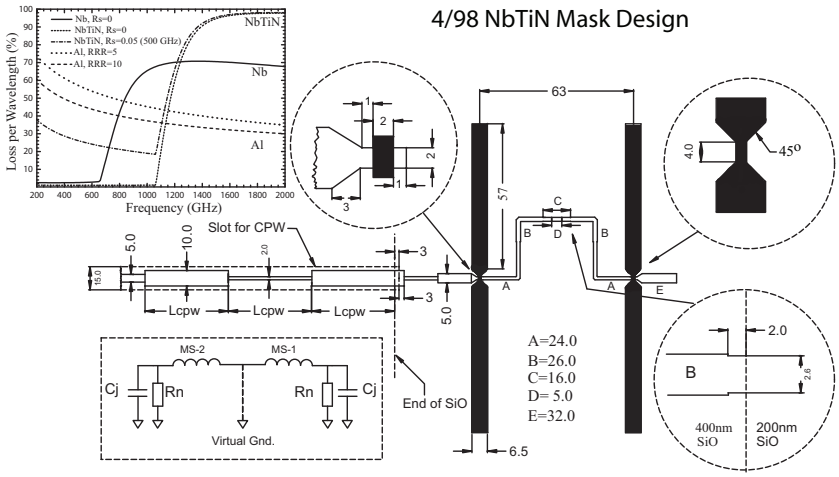

Figure 17. Layout of the all NbTiN twin-slot mixer (AlN barrier). The junction R_nA product is $20\,\Omega\,cm^2$, $J_c = 10\,kA\,cm^{-2}$. The inset shows the loss per wavelength of Nb, NbTiN, and Al films. Clearly above $\sim 700\,GHz$ the use of NbTiN is preferred. Long $0.25\,\mu m \times 2.6\,\mu m$ SIS junctions were used to minimize spreading inductance.

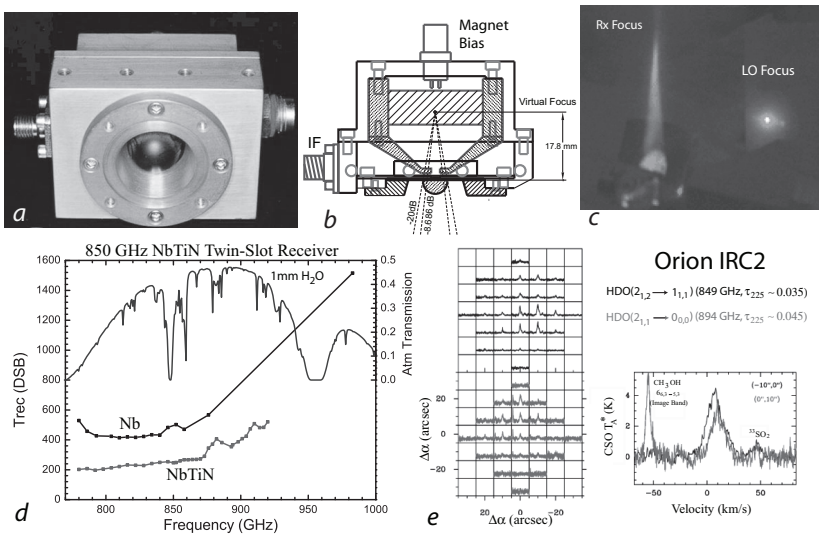

Figure 18. *a*) Front view of the twin slot mixer block. The lens material is high resistivity silicon which has been antireflection coated to minimize loss. *b*) Schematic layout of the mixer block (D. Miller et al.). *c*) Cryostat optics alignment test. *d*) Receiver DSB noise temperature (sensitivity) comparison of the Nb waveguide mixer and NbTiN twin-slot mixer. As of this writing the NbTiN twin-slot mixer remains one of the most sensitive of heterodyne mixers in this frequency range. *e*) First detection of HDO($2_{1,2} \rightarrow 1_{1,1}$) and HDO($1_{1,1} \rightarrow 0_{0,0}$) in Orion IRc2 by J. Pardo (2000). See the text for details.

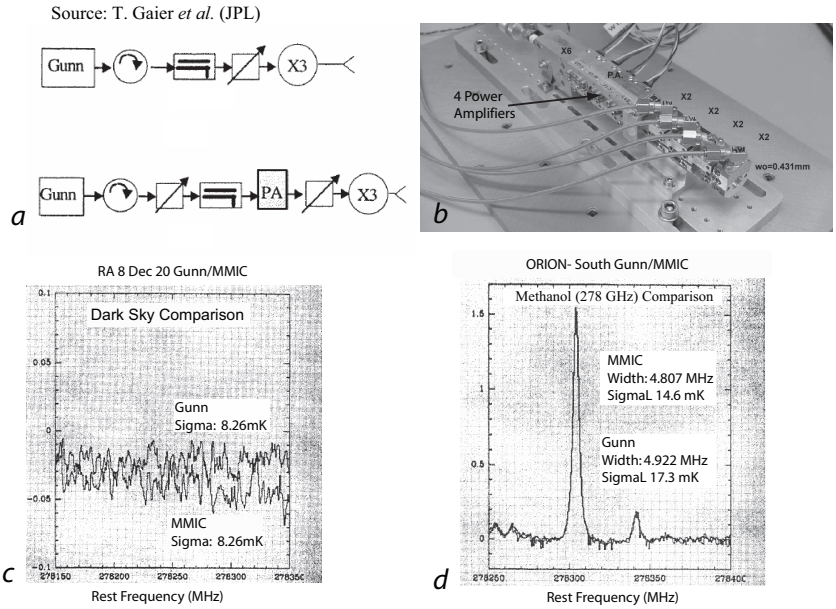

Figure 19. *a*) LO configuration with and without the JPL power amplifier. *b*) Four PA's configured in series in a HIFI (B6a) local oscillator chain. *c*) Integration on a dark piece of sky with both LO configurations. The small difference is most likely due to changing atmospheric conditions during the test. *d*) Methanol in Orion for both configurations. There is no evidence of excess (am) noise or line broadening (FM noise).

receiver of Section 3.7., as shown in Figure 18*d*, is mostly due to a reduction in the (thin) film absorption loss (Kawamura et al. 1999; Kooi et al. 2000b). Note that the all NbTiN quasi-optical mixer uses the same cooled optics, cryostat, and electronics as the 850 GHz waveguide receiver described in Section 3.7.

Among the first observations (Pardo et al. 2001) carried out with the new receiver were 10″ resolution maps of two contiguous HDO transitions: $J_{Ka,Kb} = 2_{1,2} \rightarrow 1_{1,1}$ at 848.9619 GHz, and $J_{Ka,Kb} = 1_{1,1} \rightarrow 0_{0,0}$ at 893.6387 GHz towards Orion IRc2. The weather conditions during the observing runs (January and March 2000) were excellent and provided average zenith transmissions above Mauna Kea as high as $\sim 38.5\,\%$ (849 GHz) and $\sim 42\,\%$ (886 GHz). This resulted in single sideband (SSB) system temperatures at 849 GHz as low as 1700 K at the elevation of the source (70 deg) at the beginning of the observations. Integration time for each point was 3 minutes.

3.9. W-band Power Amplifier Testing at the CSO

In 1999, with the HIFI instrument (de Graauw et al. 2006) on Herschel under serious development, it was important to show, by measurement on a telescope, that there would be no increase in noise from the use of GaAs based power amplifiers (PA) in the instrument's local oscillator chains (LOU). Again the usefulness of the CSO as a technology test-bed was demonstrated.

In a combined effort of T. Guyer (JPL), I. Mehdi (JPL), J. Pearson (JPL), R. Chamberlin (CSO), and J. Kooi, we compared in December 1999 a traditional

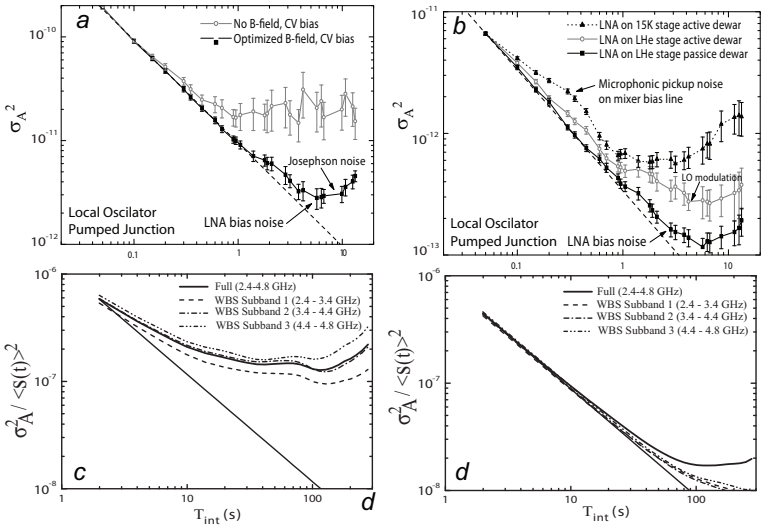

Figure 20. *a*) Total power stability of a LO pumped twin-slot mixer with and without nulling of the Josephson effect. Data was taken in a LHe cryostat. *b*) Total power stability with the low noise amplifier (LNA) mounted in a LHe cryostat and CTI cooled hybrid dewar. In the hybrid dewar the LNA was mounted in two ways; directly to the 15 K actively cooled stage and to the LHe stage. In the passive dewar Josephson instability and/or SIS bias noise induced gain instability shows up at 6 s. In the active hybrid dewar, acoustic LO modulation becomes apparent for integration times between 1 and 6 seconds. *c*) Total power stability of HIFI HEB mixer band 7 at 1.867 THz. The Allan time, in a fluctuation noise bandwidth of ~ 1.8 MHz, is ~ 8 s. *d*) Similar, but this time the spectroscopic Allan variance stability time (~ 80 s).

230 GHz $\times 3$ Gunn oscillator LO chain against one which includes a 80 – 100 GHz power amplifier (W-band). The test setup is demonstrated in Figure 19*a*. The measurement showed that a power amplifier driven by a Gunn oscillator does not introduce noticeable excess noise, as long as the amplifier is in saturation. In Figure 19*c* we compare spectra taken with the traditional, and power amplifier inserted, LO chain on dark sky. On-source integration time was approximately 15 minutes. To further investigate the effect of using a power amplifier in the LO chain, a methanol spectrum was taken towards Orion at 278 GHz. As can be observed from Figure 19*d* there is very little difference between both spectra in terms of amplitude and phase noise (broadening of the line shape).

It should be noted that the LOU on HIFI uses eighty-three power amplifiers and needless to say this demonstration, and the fact that the world did not end three weeks later, provided confidence that ultimately the planned LOU configuration was going to work. This is not to say that no local oscillator related problems were encountered. Most of these issues are however due to the use of commercial synthesized source units that have been designed for continuous frequency coverage (a Gunn oscillator is a clean fundamental source), and spurious intermodulation signals in the multipliers.

4. The 21st Century

4.1. Receiver Stability

With the start of the new millennium a new technical challenge in regards to instrument stability presented itself. Fundamentally the question was raised by Prof. R. Schieder (U. Köln), on sabbatical at Caltech in 2000: "Which component in the heterodyne receiving system is responsible, and for how much, for the so often observed instrument instability that leads to loss in integration efficiency, poor baseline quality, intensity calibration errors, and platforming effects". The urgency of this question should be seen in light of the HIFI instrument development at that time. Traditionally, receiver groups had always pointed at the backend processing units for the often observed baseline distortion, whereas the backend groups would conveniently place the blame on the front-end receiver system. But what were really the sources of instability, and how could they be best mitigated?

Again the CSO took up the challenge (and time) to investigate this important issue (Kooi et al. 2000a). The root of the problem was found to lie primarily with the front-end SIS (HEB) mixer, local oscillator, groundloops, microphonics, thermal instability, bias electronics, and Josephson noise, much to the relief of Prof. Schieder who is well known for his group's excellent wideband acousto-optical spectrometer backends (Schieder 1985; Schieder et al. 2000; Schieder & Kramer 2001). The result of this research is shown in Figures 20*a* and 20*b*.

As it turns out, this work has had a global impact on the way heterodyne receivers are characterized, thereby significantly improving the quality of the observations. In particular, due to the limited liquid helium (LHe) lifetime and large cost of the Herschel Space Observatory (HSO), much attention has been given to optimize observing efficiency and baseline quality for the large number of observing modes (Ossenkopf 2008) of the HIFI instrument. In Figures 19*c* and 19*d* we show two stability examples taken during the thermal balanced and thermal vacuum tests (TB/TV) at Estec, Noordwijk (The Netherlands), in November 2008. Details are in the caption.

For the CSO, the knowledge gained from this experience feeds back into the planned heterodyne instrument upgrade (Kooi et al. 2003). Improved continuum and spectroscopic stability is of importance for a large variety of scientific investigations, not the least of which was the study of beam diluted high redshift extragalactic objects.

4.2. High Current Density SIS Mixers

The 850 GHz twin slot device of section 3.8. utilized thin film NbTiN wire and ground layers. Since it has proven difficult to grow a high quality epitaxial NbTiN top layer at a sufficiently low temperature, so as not to degrade the junction trilayer, future devices were to use aluminum for the top wire layer. However, this solution poses a problem in that Al is not a superconductor at the temperatures and frequencies at which the SIS mixers are operated. A convenient way to mitigate this problem and minimize the effect of absorption loss in the (microstrip) RF matching network, located between the antenna and SIS junction, is to increase the critical-current density of the SIS junction, thereby increasing the fractional power coupled to it.

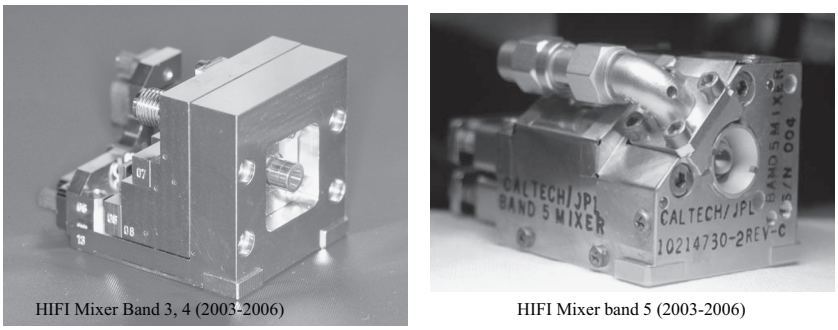

Figure 21. *Left:* The HIFI band 4 waveguide mixer. The RF operating frequency is 960 – 1120 GHz. The SIS mixer uses a NbTiN ground layer, Al wire layer and a $Nb/AlO_2/Nb$ trilayer with a critical current density of $6.5\,kA\,cm^{-2}$. The quality factor (R_{sg}/R_n) is very high, ~ 40. *Right:* HIFI mixer band 5. The antenna layout is of the twin-slot type shown in Figure 17, the critical-current density $30\,kA\,cm^{-2}$, and the junction area $0.25\,\mu m^2$. The SIS mixer uses a Nb-AlN-NbTiN trilayer with a 3.5 mV gap voltage and a Nb ground- and Al wire layer.

Fortunately aluminum-nitride tunnel barriers (Shiota, Imamura, & Hasuo 1992), unlike aluminum-oxide barriers which have a practical (quality) upper limit of $\sim 20\,kA\,cm^{-2}$, allow higher current densities for similar barrier thicknesses. It is in fact also possible to reduce the barrier thickness while maintaining junction quality. AlN barrier technology has been demonstrated to produce SIS junctions with critical-current densities upwards of $70\,kA\,cm^{-2}$ (Zijlstra et al. 2007) and thus lends itself well for terahertz SIS mixers applications. As noted, the NbTiN film and AlN barrier development has in large part been driven by the need to develop sensitive heterodyne mixers for HIFI (de Graauw et al. 2006) band 4 (960 – 1120 GHz, Jackson et al. 2006) and HIFI band 5 (1116 – 1272 GHz, Karpov et al. 2004). In Figure 21*a* we depict the HIFI band 4 waveguide mixer (SRON[9]), and in Figure 21*b* the band 5 quasi-optical twin-slot SIS mixer developed at Caltech/JPL.

4.3. The Technology Development Receiver (Trex)

The CSO, in need of tunerless wide IF bandwidth receivers, conveniently baselined the high critical-current density AlN barrier development for a set of balanced receivers that span the 180 – 720 GHz frequency range. The twin-junction design by Kovács (Kooi et al. 2007) is shown in Figure 22, and employs high current density ($J_c = 25\,kA\,cm^{-2}$) Nb/AlN/Nb tunnel junctions. The low ωRC product of these junctions affords an unprecedented 45 % instantaneous RF bandwidth. To provide a similarly large fractional coupling to a full height waveguide, the asymmetric radial probe design by Withington et al. (1999; see Kooi et al. 2003) is used. A further feature of the new chip design is that a thin film capacitor has been integrated on chip to extend the IF bandwidth to 13 GHz. Extensive Tucker based (Tucker & Feldman 1985) superconducting

[9]SRON, Netherlands Institute for Space Research.

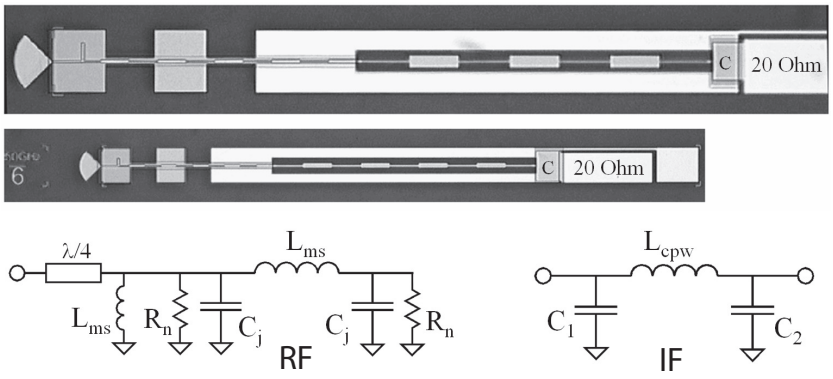

Figure 22. 350 GHz junction layout. The radial probe antenna is visible on the left side. The IF signal is taken out via a microstrip RF choke (on 300 nm SiO, ε_r=5.6) that connects to a high impedance CPW transmission line (inductive) and integrated shunt capacitor (C). This L-C mechanism provides a π tuning network with the combined capacitance of the probe, twin-junction RF tuning structure, and microstrip RF matching network (C). The passband is optimized to cover 1 – 13 GHz. To minimize gain compression, the integrated shunt capacitor also serves to terminate out-of-band broadband noise. The IF impedance presented to the twin SIS junctions is 14 Ω, $\sim 2.7\,R_n$.

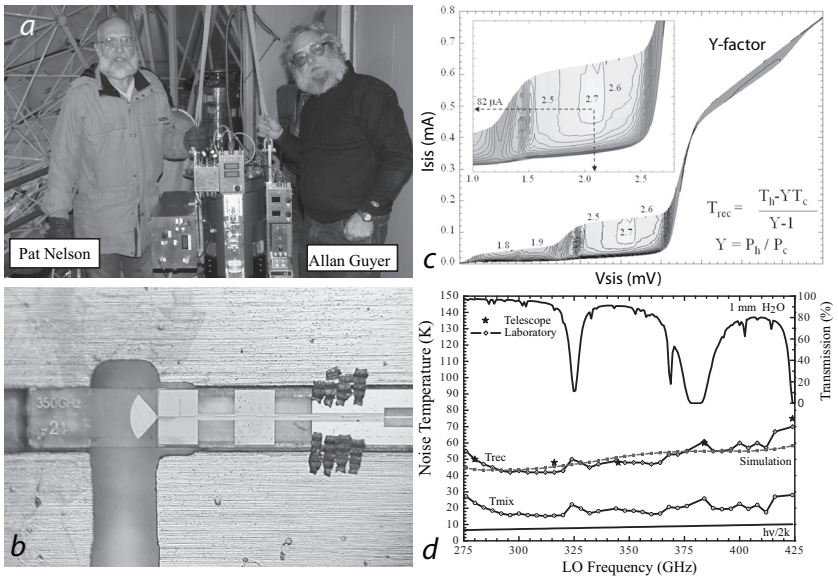

Figure 23. *a*) Pat Nelson and Allan Guyer hoisting the 280 – 420 GHz 'Technology development receiver' (Trex) onto the telescope. *b*) Close-up view of the 345 GHz chip mounted in the waveguide. Note the broadband asymmetric radial probe design. *c*) Optimal Y-factor at 345 GHz as a function of bias voltage and LO pump level. *d*) Receiver noise temperature as a function of frequency.

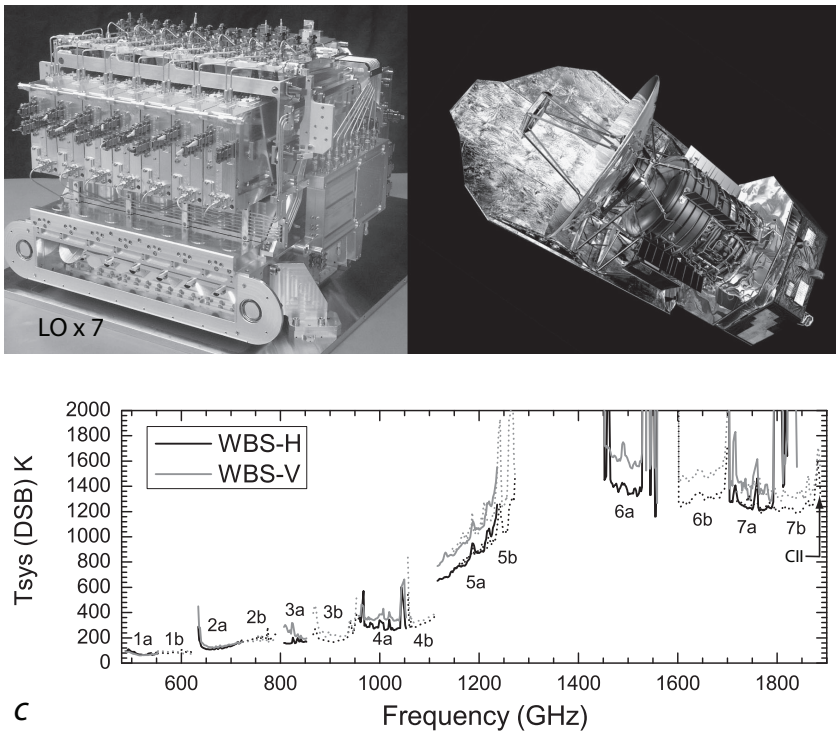

Figure 24. *a*) The HIFI instrument. There are seven frequency bands, covering the 480 GHz – 2 THz frequency range in nearly continuous fashion. Each band consists of two mixers, sensitive to either the H or V polarization. Visible towards the bottom left are the seven input ports through which the LO beams for each of the mixer bands is coupled. *b*) Rendition of the Herschel observatory. *c*) Measured system noise temperature during the Checkout Phase (CoP). The occasional spikes are due to a lack of LO pump power (Courtesy D. Teyssier, ESOC).

mixer calculations were performed in Supermix (Ward et al. 1999), a flexible software library for high-frequency harmonic-balanced mixer and superconducting circuit simulations.

In 2003 the newly designed high current density AlN-barrier SIS junctions were fabricated at the micro device laboratory (JPL) by B. Bumble. The wafer layout contains four configurations, each with three design variations, spanning the 180 – 720 GHz atmospheric windows. Being operated below the Nb energy gap ($\sim$ 690 GHz), both the ground and top layer films could be made of this material (T_c = 9.2 K). After lapping the Z-cut quartz wafers to 50 μm (from an original thickness of 250 μm) by a commercial company, and dicing of the wafers at JPL (spring 2004), it was decided to construct a single-ended DSB receiver in the 280 – 420 GHz frequency range. This would help verify the variety of new technologies. The 'Technology development receiver' (Kooi et al. 2007), or Trex, was installed at the CSO in 2007. Shown in Figure 23*a* are Pat Nelson (electronics technician) and Allan Guyer (mechanic) in the process of hoisting Trex onto the relay optics (Serabyn 1997) in the Cassegrain focus area of the telescope. Figure 23*b* shows a close up of the junction and radial

probe mounted in the waveguide. The optimum Y-factor response is shown in Figure 23*c* with the corresponding receiver noise temperature as a function of frequency in Figure 23*d*.

4.4. The High Frequency Instrument (HIFI) on the Herschel Space Observatory

The next big event was the launch of the Herschel (de Graauw & Helmich 2001) space observatory on 14 May 2009. HIFI, the high spectral resolution ($R \geq 10^6$) heterodyne instrument on Herschel has been in the making for 10 years (T. G. Phillips is the US principal investigator), and has, as we have seen, benefited significantly from technology development at Caltech, JPL, and the CSO. In Figure 24*a* we show a photograph of the HIFI instrument. HIFI covers the 480 GHz – 2 THz frequency range and consists of seven dual-polarized mixer bands. The local oscillator unit consists of eighty-three power-amplifiers (subsection 3.9.) and fourteen multiplier chains (not shown). IF backend processing is done by means of a 2 GHz wide high resolution digital correlator (Belgacem et al. 2004) and a 4 GHz wide acousto-optical spectrometer (Schieder et al. 2000), one for each polarization. Figure 24*b* is a photograph of a Herschel model. Herschel's primary mirror is 3.5 m, the largest single mirror ever flown into space. The commissioning phase (CoP) measured system noise temperatures are shown in Figure 24*c*. Mixer band 5 was made at Caltech/JPL (Karpov et al. 2004). The occasional sharp rise in noise temperature is due to a lack of LO oscillator power. By putting astronomical lines in either the USB or LSB complete coverage is obtained in the specified bands.

5. The Near Future

So far we have only looked at the past and present. It is therefore productive to have a brief look into the (short term) CSO future. Even though the CSO is slated to be closed around 2016, it remains of scientific importance to upgrade the somewhat aging heterodyne receivers. It will also benefit CCAT (Radford et al. this volume), the 25 m Caltech Cornell Atacama telescope slated to be built on Cerro Chajnantor, Chile, and inaugurated around the same time. To this end we have designed four balanced receivers covering the 180 – 720 GHz atmospheric windows. In addition a specialized 280 – 420 GHz balanced autocorrelation, or continuous comparison receiver with two $2'$ offset pixels on the sky, one for the on-source position and one for the off-source position, is also under construction. The primary science goals are high-redshift extragalactic molecular and atomic line spectroscopy. The continuous differencing should allow for very deep integrations, on the order of 120 μK (1σ) in 8 hours at the CSO (Kooi et al. 2003).

The advantage of the balanced receivers design is that this type of configuration offers a high degree of amplitude (am) noise rejection. In the case of the new CSO receivers am noise rejection is estimated to be approximately 13 – 15 dB. With the advent of synthesized local oscillators this feature is expected to be of considerable importance. Another advantage of balanced receivers is the fact that all available LO power is utilized, thus facilitating wide RF bandwidth performance. Of course the balanced receiver remains of the DSB type. Ideally

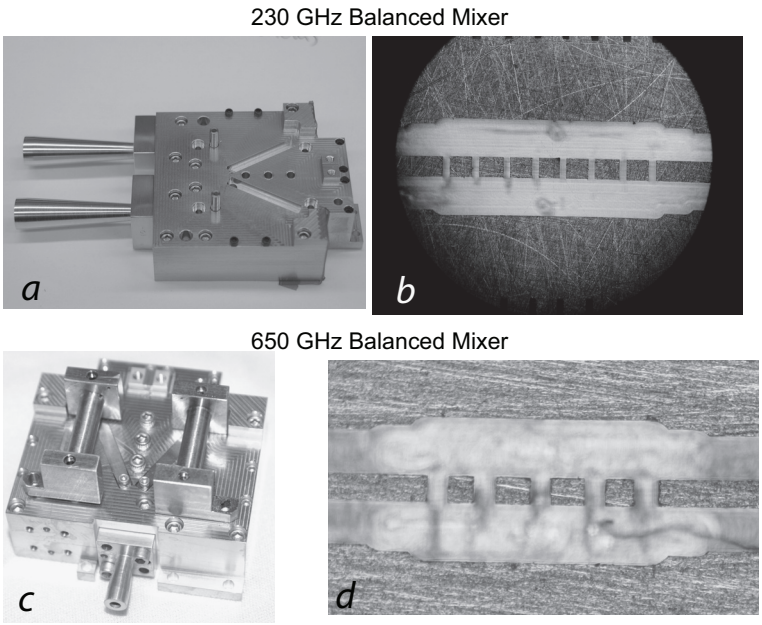

Figure 25. *a*) The 230 GHz balanced mixer. The LO feedhorn is in reality removed to allow LO injection via a waveguide coupling section (not shown). *b*) A close up view of the 230 GHz quadrature hybrid. *c*) A 650 GHz balanced mixer. Note the smaller side corrugated feedhorn. *d*) The 650 GHz 90° hybrid. For details see (Kooi et al. 2003).

a balanced sideband separating mixer is used, having the property of canceling atmospheric noise in one of the sidebands while simultaneously providing amplitude noise cancellation of the local oscillator. In Figure 25*a* we show a photograph of the 230 GHz balanced mixer (CMI) with the quadrature hybrid shown in Figure 25*b*. Figures 25*c* and 25*d* show the 650 GHz mixer.

To maximize science, and allow pointing with the 460 and 650 GHz mixers under mediocre weather conditions, two-color observations are planned for the 230/460 GHz and 345/650 GHz atmospheric windows. Figure 26 shows a rendition of the 345/650 GHz two-color receiver. A wire grid on the LHe stage is used to separate the circular polarized sky signal into two linear components. The H-polarized signal is routed to the 345 GHz mixer with the V-polarization routed to the 650 GHz mixer. The LO multiplier is physically mounted to the LHe stage but thermally connected to the 15 K shield.

The multiplier output signal is connected to the mixer LO port via a custom waveguide and fixed-tuned (course setting) attenuator. Note that the 230/460 GHz dual-color balanced configuration is identical to the one described here. Procurement of all hardware is now complete and full assembly of the 230/460 GHz cryostat is expected in Fall 2009.

In Figure 27 we depict the simulated balanced receiver noise temperatures. Overlaid is the measured 'Technology Development Receiver' noise temperature of Section 4.3. Note the good agreement between measurement and simulation (Ward et al. 1999). The difference in amplitude between the 280 – 420 GHz balanced receiver and Trex is due to the way the local oscillator signal is injected.

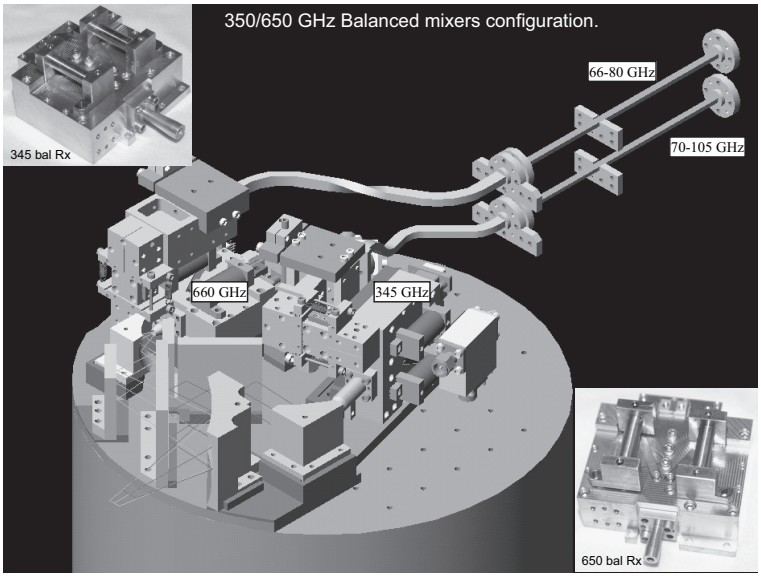

Figure 26. Rendering of the 345/650 GHz two-color receiver. The multiplier is physically mounted on the LHe stage, but thermally connected to the 15 K shield. The two-color separation is achieved via a cooled wire grid. The advantages of this configuration are several: Pointing with the high frequency receiver in mediocre weather and twice the science throughput on a good night. The 230/460 GHz cryostat has a very similar layout.

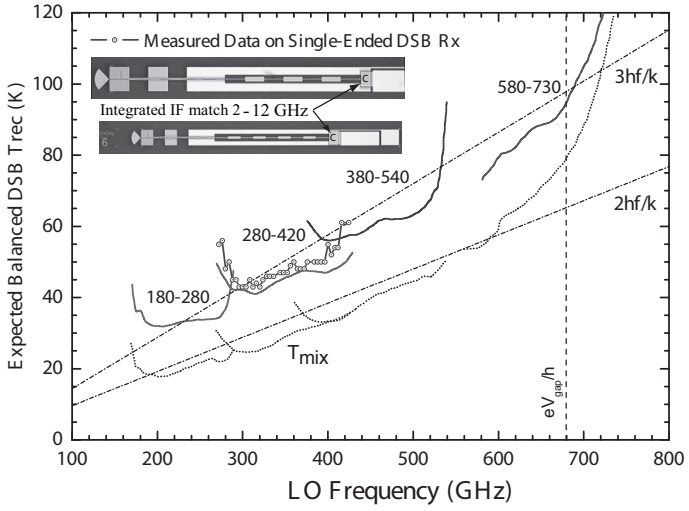

Figure 27. Calculated balanced receiver noise temperature vs. measured Trex data. The difference in amplitude between the 280 – 420 GHz balanced receiver and Trex is due to the am noise cancellation properties of the balanced mixer. *Inset*) 460 and 650 GHz AlN-barrier junctions on 50 μm quartz with integrated IF matching network.

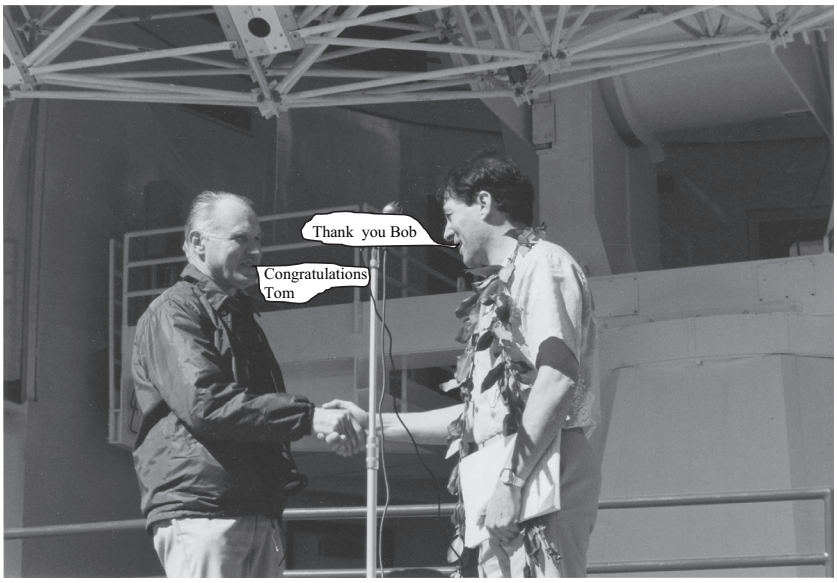

Figure 28. Prof. R. Leighton (left) and Prof. T. G. Phillips at the November 1987 inauguration ceremony of the CSO. If Bob Leighton were still alive today he would say something like this.

6. Conclusion

In this article we have taken a look at the rich history of heterodyne receiver development at the CSO. Spurred by the quest for high spectral resolution galactic and extragalactic atomic and molecular spectroscopy, a tremendous technological development in terms of sensitivity, instantaneous RF and IF bandwidth, frequency coverage, instrument stability and LO automation has taken place in the last twenty years. The CSO and Prof. T. G. Phillips have certainly played major parts in this development. The observatory's hands-on and flexible approach, all the while in pursuit of scientific excellence, certainly provided an environment where technological breakthroughs and (astro)physics experiments were made possible.

This is the legacy of Prof. Phillips. If Bob Leighton were still alive he would certainly congratulate Tom for this most excellent achievement (Fig. 28).

Acknowledgments. Countless people have been involved in the CSO during the last 20+ years. The story presented here has focused on the heterodyne receiver development at the CSO with associated technological spin-offs. Needless to say, this does not address the large contribution from the direct detection (flux) and cosmology community. Every effort has been made to be historically accurate and to credit the work of colleagues where applicable. For those who go unmentioned we would like to thank you for your contributions in making the CSO what it is. This work was supported in part by NSF Grants AST 05-40882 and AST 08-38261.

References

Bardeen, J., Cooper, L. N., & Schrieffer, J. R. 1957, Phys. Rev., 108, 1175
Belgacem, M., Ravera, L., Caux, E., Caïs, P., & Cros, A. 2004, New Astron., 9, 43
Belitsky, V. Y., Tarasov, M. A., Kovtonjuk, S. A., Filippenko, L. V., & Kaplunenko, O. V. 1992, Int. J. IR & MM Waves, 13, 389
Bin, M. 1997, PhD thesis, California Institute of Technology, Pasadena, CA
Blake, G. A., Masson, C. R., Phillips, T. G., & Sutton, E. C. 1986, ApJS, 60, 357
Buttgenbach, T. H., Watson, D. M., Phillips, T. G., Miller, R. E., & Wengler, M. J. 1988, IEEE Trans. Microw. Theor. Tech., 36, 1720
Dayem, A. H. & Martin, R. J. 1962, Phys. Rev. Lett., 8, 246
de Graauw, T. & Helmich, F. P. 2001, in ESA Special Publication, Vol. 460, The Promise of the Herschel Space Observatory, ed. G. L. Pilbratt, J. Cernicharo, A. M. Heras, T. Prusti, & R. Harris, 45, www.astro.phys.ethz.ch/herschel/HerschelHifi.pdf
de Graauw, Th., Whyborn, N., Caux, E., Phillips, T. G., Stutzki, J., Tielens, X., Güsten, R. G., Helmich, F. P., Luinge, W., Pearson, J., Roelfsema, P., Schieder, R., Wildeman, K., & Wavelbakker, K. 2006, Online: herschel.esac.esa.int/Publ/2006/SPIE2006_HIFI_paper.pdf
de Lange, G., Honingh, C. E., Kuipers, J. J., Schaeffer, H. H. A., Panhuyzen, R. A., Klapwijk, T. M., van de Stadt, H., & de Graauw, M. M. W. M. 1994, Appl. Phys. Lett., 64, 3039
Dolan, G. J., Linke, R. A., Sollner, T. C. L. G., Woody, D. P., & Phillips, T. G. 1981, IEEE Trans. Microw. Theor. Tech., 29, 87
Dowell, C. D. et al. 2003, in SPIE Conf. Ser., Vol. 4855, Millimeter and Submillimeter Detectors for Astronomy, ed. T. G. Phillips & J. Zmuidzinas, 73
Ellison, B. N. & Miller, R. E. 1987, Int. J. IR & MM Waves, 8, 609
Ellison, B. N., Schaffer, P. L., Schaal, W., Miller, R. E., & Vail, D. 1989, Int. J. IR & MM Waves, 10, 937
Gaidis, M., LeDuc, H. G., Bin, M., Millera, D., Stern, J. A., & Zmuidzinas, J. 1996, IEEE Trans. Microw. Theor. Tech., 44, 1130
Gillespie, A. R. & Phillips, T. G. 1979, A&A, 73, 14
Groppi, C. et al. 2006, in SPIE Conf. Ser., Vol. 6275, Millimeter and Submillimeter Detectors and Instrumentation for Astronomy III, ed. J. Zmuidzinas, W. S. Holland, S. Withington, & W. D. Duncan, 62750O
Jackson, B. D., de Lange, G., Zijlstra, T., Kroug, M., Kooi, J. W., Stern, J. A., & Klapwijk, T. M. 2006, IEEE Trans. Microw. Theor. Tech., 54, 547
Josephson, B. D. 1962, Phys. Lett., 1, 251
Karpov, A., Miller, D., Rice, F. R., Stern, J. A., Bumble, B., LeDuc, H. G., & Zmuidzinas, J. 2004, in SPIE Conf. Ser., Vol. 5498, Millimeter and Submillimeter Detectors for Astronomy II, ed. J. Zmuidzinas, W. S. Holland, & S. Withington, 616
Kawamura, J., Chen, J., Miller, D., Kooi, J., Zmuidzinas, J., Bumble, B., Leduc, H. G., & Stern, J. A. 1999, Appl. Phys. Lett., 75, 4013
Keene, J., Schilke, P., Kooi, J., Lis, D. C., Mehringer, D. M., & Phillips, T. G. 1998, ApJ, 494, L107
Kooi, J. W. 2008, PhD thesis, Rijksuniversiteit Groningen, NL
Kooi, J. W., Chan, M., Bumble, B., LeDuc, H. G., Schaffer, P., & Phillips, T. G. 1995, Int. J. IR & MM Waves, 16, 2049
Kooi, J. W., Chan, M., Phillips, T. G., Bumble, B., & Leduc, H. G. 1992, IEEE Trans. Microw. Theor. Tech., 40, 812
Kooi, J. W., Chattopadhyay, G., Thielman, M., Phillips, T. G., & Schieder, R. 2000a, Int. J. IR & MM Waves, 21, 689
Kooi, J. W., Chattopadhyay, G., Withington, S., Rice, F., Zmuidzinas, J., Walker, C., & Yassin, G. 2003, Int. J. IR & MM Waves, 24, 261
Kooi, J. W. et al. 2000b, Int. J. IR & MM Waves, 21, 1357

Kooi, J. W., Kovacs, A., Kaye, S. M., Dama, J., Edgar, M. L., Zmuidzinas, J., & Phillips, T. G. 2003, in SPIE Conf. Ser., Vol. 4855, Millimeter and Submillimeter Detectors for Astronomy, ed. T. G. Phillips & J. Zmuidzinas, 265
Kooi, J. W. et al. 2007, IEEE Trans. Microw. Theor. Tech., 55, 2086
Kooi, J. W., Pety, J., Bumble, B., Walker, C. K., LeDuc, H. G., Schaffer, P. L., & Phillips, T. G. 1998, Int. J. IR & MM Waves, 46, 151
Kooi, J. W., Chan, M. S., Leduc, H. G., & Phillips, T. G. 1996, Proc. 7^{th} Int. Symp. Space Terahertz Technology, Charlottesville, Va, Mar
Ossenkopf, V. 2008, A&A, 479, 915
Padin, S. & Ortiz, G. G. 1991, IEEE Trans. Microw. Theor. Tech., 39, 1239
Pardo, J. R., Cernicharo, J., Herpin, F., Kawamura, J., Kooi, J., & Phillips, T. G. 2001, ApJ, 562, 799
Phillips, T. G. 2007, in IEEE/MTT-S Int. Microw. Symp., 1849
Phillips, T. G. & Keene, J. 1992, IEEE Proc., 80, 1662
Phillips, T. G. & Woody, D. P. 1982, ARA&A, 20, 285
Radford, S. J. E., Giovanelli, R., Sebring, T. A., & Zmuidzinas, J. this volume
Rutledge D. B., Neikirk D. P., & Kasilingam D. P. 1984, Int. J. IR & MM Waves, 10, 1
Salez, M., Febvre, P., Mcgrath, W. R., Bumble, B., & Leduc, H. G. 1994, Int. J. IR & MM Waves, 15, 349
Schieder, R. 1985, in SPIE Conf. Ser., Vol. 598, Instrumentation for Submillimeter Spectroscopy, ed. E. L. Kollberg
Schieder, R. & Kramer, C. 2001, A&A, 373, 746
Schieder, R. T., Siebertz, O., Schloeder, F., Gal, C., Stutzki, J., Hartogh, P., & Natale, V. 2000, in SPIE Conf. Ser., Vol. 4013, UV, Optical, and IR Space Telescopes and Instruments, ed. J. B. Breckinridge & P. Jakobsen, 313
Schilke, P., Benford, D. J., Hunter, T. R., Lis, D. C., & Phillips, T. G. 2001, ApJS, 132, 281
Schoelkopf, R. 1994, PhD thesis, California Institute of Technology, Pasadena, CA
Schuster, K. F., Harris, A. I., & Gundlach, K. H. 1993, Int. J. IR & MM Waves, 14, 1867
Serabyn, E. 1997, Int. J. IR & MM Waves, 18, 273
Shapiro, S. & Little, A. D. 1963, Phys. Rev. Lett.
Shiota, T., Imamura, T., & Hasuo, S. 1992, Appl. Phys. Lett., 61, 1228
Sutton, E. C. 1983, IEEE Trans Microw. Theor. Tech., 31, 589
Sutton, E. C., Blake, G. A., Masson, C. R., & Phillips, T. G. 1985, ApJS, 58, 341
Tucker, J. R. 1979, IEEE J. Quantum Electron., 15, 1234
Tucker, J. R. & Feldman, M. J. 1985, Rev. Mod. Phys., 57, 1055
Walker, C. K., Kooi, J. W., Chant, M., Leduc, H. G., Schaffer, P. L., Carlstrom, J. E., & Phillips, T. G. 1992, Int. J. IR & MM Waves, 13, 785
Wang, N. et al. 1996, Appl. Optics, 35, 6629
Ward, J., Rice, F., Chattopadhyay, G., & Zmuidzinas, J. 1999, in 10^{th} Int. Symp. Space Terahertz Tech., ed. T. W. Crowe & R. M. Weikle, 268
Wengler, M. J. & Woody, D. P. 1987, IEEE J. Quantum Electron., 23, 613
Wengler, M. J., Woody, D. P., Miller, R. E., & Phillips, T. G. 1985, Int. J. IR & MM Waves, 6, 697
Withington, S., Yassin, G., Leech, J., & Isaak, K. G. 1999, in Tenth International Symposium on Space Terahertz Technology, 508
Woody, D. P., Giovanine, C. J., & Miller, R. E. 1989, IEEE Trans. Magnetics, 25, 1366
Woody, D. P., Wengler, M. J., & Miller, R. E. 1985, IEEE Trans. Microw. Theor. Tech., 33, 90
Zijlstra, T., Lodewijk, C. F. J., Vercruyssen, N., Tichelaar, F. D., Loudkov, D. N., & Klapwijk, T. M. 2007, Appl. Phys. Lett., 91, 233102
Zmuidzinas, J., Kooi, J. W., Kawamura, J., Chattopadhyay, G., Bumble, B., Leduc, H. G., & Stern, J. A. 1998, in SPIE Conf. Ser., Vol. 3357, Advanced Technology MMW, Radio, and Terahertz Telescopes, ed. T. G. Phillips, 53

Zmuidzinas, J. & LeDuc, H. 1992, IEEE Trans. Microw. Theor. Tech., 40, 1797
Zmuidzinas, J., Leduc, H. G., Stern, J. A., & Cypher, S. R. 1994, IEEE Trans. Microw. Theor. Tech., 42, 698

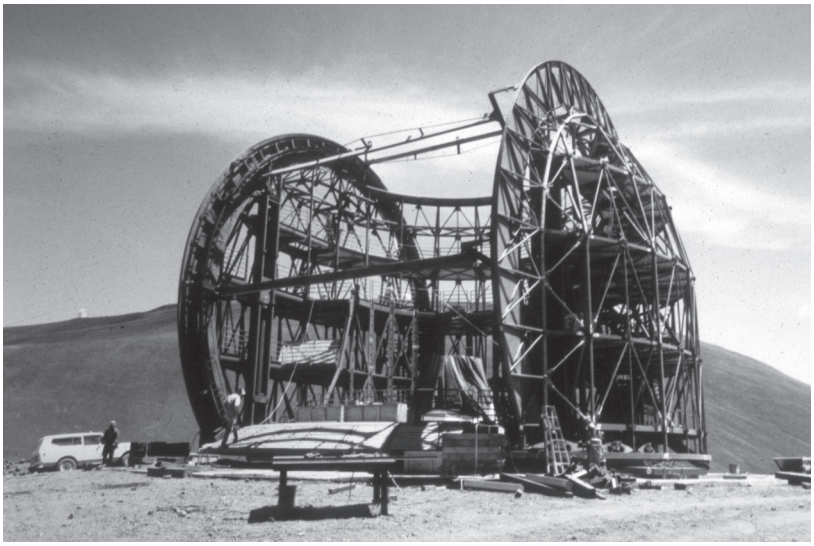

Construction of the Caltech Submillimeter Observatory atop Mauna Kea in Hawaii (ca. 1985)